Properties and evolution of biomass burning organic aerosol from Canadian boreal forest fires

M. D. Jolleys[1], H. Coe[1], G. McFiggans[1], J. W. Taylor[1], S. J. O'Shea[1], M. Le Breton[1], S. J.-B. Bauguitte[2], S. Moller[3], P. Di Carlo[4,5], E. Aruffo[4,5], P. I. Palmer[6], J. D. Lee[3]

[1] {Centre for Atmospheric Science, School of Earth, Atmospheric and Environmental Science, University of Manchester, Manchester, UK}

[2] {Facility for Airborne Atmospheric Measurements, Bedford, UK}

[3] {National Centre for Atmospheric Science (NCAS), Department of Chemistry, University of York, York, UK}

[4] {Centre of Excellence CETEMPS, University of L'Aquila, L'Aquila, Italy}

[5] {Department of Physical and Chemical Sciences, University of L'Aquila, L'Aquila, Italy}

[6] {School of Geosciences, University of Edinburgh, Edinburgh, UK}

Corresponding to: M. D. Jolleys (matthew.jolleys@manchester.ac.uk)

Abstract

Airborne measurements of biomass burning organic aerosol (BBOA) from boreal forest fires reveal highly contrasting properties for plumes of different ages. These measurements, performed using an Aerodyne Research Inc. compact time-of-flight aerosol mass spectrometer (C-ToF-AMS) during the BORTAS (quantifying the impact of BOReal forest fires on Tropospheric oxidants over the Atlantic using Aircraft and Satellites) experiment in the summer of 2011, have been used to derive normalised excess organic aerosol (OA) mass concentrations ($\triangle$OA/$\triangle$CO), with higher average ratios observed closer to source (0.190 ± 0.010) than in the far-field (0.097 ± 0.002). The difference in $\triangle$OA/$\triangle$CO between fresh and aged plumes is influenced by a change in dominant combustion conditions throughout the campaign. Measurements at source comprised 3 plume interceptions during a single research flight and sampled largely smouldering fires. 23 interceptions were made across 4 flights in the far-field, with plumes originating from fires occurring earlier in the campaign when fire activity had been more intense, creating an underlying contrast in emissions prior to any transformations associated with aging. Changing combustion conditions also affect the vertical distribution of biomass burning emissions, as aged plumes from more flaming-dominated fires are injected to higher altitudes of up to 6000 m. Proportional contributions of the mass-to-charge ratio (*m*/*z*) 60 and 44 peaks in the AMS mass spectra to the total OA mass (denoted f_{60} and f_{44}) are used as tracers for primary and oxidized BBOA, respectively. f_{44} is lower on average in near-field plumes than those sampled in the far-field, in accordance with longer aging times as plumes are transported a greater distance from source. However, high levels of $\triangle O_3/\triangle CO$ and $-\log(NO_x/NO_y)$ close to source indicate that emissions can be subject to very rapid oxidation over short timescales. Conversely, the lofting of plumes into the upper troposphere can lead to the retention of source profiles after transportation over extensive temporal and spatial scales, with f_{60} also higher on average in aged plumes. Evolution of OA composition with aging is comparable to observations of BB tracers in previous studies, revealing a consistent progression from f_{60} to f_{44}. The elevated levels of oxygenation in aged plumes, and their association with lower average $\triangle$OA/$\triangle$CO, are consistent with OA loss through evaporation during aging due to a combination of dilution and chemical

42 processing, while differences in combustion conditions throughout the campaign also have a
43 significant influence on BBOA production and composition.

1. Introduction

The BORTAS (quantifying the impact of BOReal forest fires on Tropospheric oxidants over the Atlantic using Aircraft and Satellites) campaign was a major international research effort to improve understanding of the properties and evolution of biomass burning (BB) plumes. BB emissions form a major source of atmospheric particulate matter on a global scale, contributing around 90% of the total primary organic aerosol (OA) (*Bond et al., 2004*). The radiative effects of atmospheric aerosols represent one of the major sources of uncertainty with regard to influences on climate change (*Textor et al., 2006; Forster et al., 2007*). Given the prominence of OA in global aerosol budgets (*Zhang et al., 2007; Jimenez et al., 2009*), limited understanding of BB emissions, and more specifically biomass burning organic aerosol (BBOA) emissions, forms an important component of this uncertainty. Improved projection of climate change impacts through global climate model simulation is dependent on more robust parameterisation of the constituent drivers, constrained by direct measurements. Several fundamental aspects of the BBOA lifecycle remain poorly characterised (*Hallquist et al., 2009*), including the conditions and processes controlling formation and the effects of transformations occurring during aging, such as gas-particle partitioning of low volatility organic compounds following photo-oxidation, heterogeneous reactions with existing OA and losses through dilution-based evaporation or volatilisation (*Reid et al., 2005; Grieshop et al., 2009; DeCarlo et al., 2010; Hennigan et al., 2011*). Variability at source has been shown to be extensive, in response to changes in both fuel properties and combustion conditions (*McMeeking et al., 2009; Jolleys et al., 2012; 2013*). The importance of secondary organic aerosol (SOA) in aging plumes is also particularly unclear. Substantial SOA formation as a result of photochemical processing has been demonstrated in laboratory experiments, increasing OA concentrations by up to a factor of 4 over several hours (*Grieshop et al., 2009; Hennigan et al., 2011; Heringa et al., 2011*). However, under ambient conditions the importance of SOA addition relative to primary (POA) emissions is more disputable. Despite widespread evidence for the increasing oxygenation of BBOA with aging (*Capes et al., 2008; DeCarlo et al., 2008; Cubison et al., 2011; Jolleys et al., 2012*), net mass enhancements are not observed consistently. The underlying causes of this variable SOA

contribution, including the implications of initial OA composition, also remain ambiguous and require further refinement.

The BORTAS campaign is described in detail by *Palmer et al.* (*2013*), with an overview of measurements used within this analysis given here. BORTAS took place across several regions of Canada between the 12th July and 3rd August in both 2010 and 2011, although activity during the 2010 deployment (BORTAS-A) was limited to ground-based measurements at a main ground station located at Dalhousie University in Halifax, Nova Scotia, along with ozonesonde launches from a network of seven sites across central and eastern Canada and supporting satellite observations (*Parrington et al., 2012*). Airborne measurements were carried out during BORTAS-B in 2011, providing all data contributing towards this study. The UK Facility for Airborne Atmospheric Measurements (FAAM) BAe-146 Atmospheric Research Aircraft (ARA) performed a total of 15 flights, including 11 dedicated science flights between the 15th and 31st July. Research flights primarily originated from Halifax and largely involved surveying areas adjacent to the Gulf of St. Lawrence and the North Atlantic. A predominant source region in northwestern Ontario (approximately 52.5° N, 93.5° W) has been identified for the majority of plumes sampled throughout BORTAS, although more disperse fires were also active in northern Alberta and the Northwest Territories (*Palmer et al., 2013; Parrington et al., 2013*). As the majority of plumes from fires in this region were encountered at a distance of several thousand kilometres downwind, emissions would have undergone substantial processing prior to sampling, with estimated photochemical ages between 1-11 days. A single flight to the Ontario source region also sampled active fires directly at source, providing a valuable inventory of fresh plume measurements and enabling comparison of emissions in the near and far-field. Tracks of all flights included within this analysis are shown in Figure 1. Back trajectories for air masses encountered throughout the durations of flights B621-624 are presented by *O'Shea et al.* (*2013$_a$*), detailing the transport pathways of plumes and agreement with active fire locations, while *Taylor et al.* (*2014*) provide air mass histories for individual plumes sampled during flight B626. Comparison of emissions of different ages is subject to potential contrasts in fire behaviour, given that each set of measurements were obtained at different stages of the campaign. Fire activity within the region peaked between the 17th and 19th July (Figure 2), with emissions from

these fires intercepted far downwind. Plumes from active fires within this region were also sampled at source on the 26th July (flight B626), representing the only measurements of fresh plumes from BORTAS. However, by this time fire activity had significantly abated, bringing about a change in combustion conditions to yield smaller, less intense fires more typically dominated by smouldering combustion (*O'Shea et al., 2013$_a$*). The more intense period of fires earlier in the campaign is expected to involve larger events with a more prominent flaming combustion phase, as indicated by the detection of pronounced smoke plumes at altitudes of up to approximately 7000 m over the North Atlantic (*Palmer et al., 2013*). As a result, any comparison of fresh and aged plumes during BORTAS must also account for this disparity in source conditions. While such a scenario would reduce the potential to evaluate the continuous evolution of smoke plumes from source into the ambient atmosphere, and prevent direct comparison of near and far-field plumes derived from similar combustion conditions, it also provides a baseline for conditions at source.

2. Background

2.1 Instrumentation and measurements

A wide array of instrumentation performing particulate and gas phase measurements were deployed throughout BORTAS. This study focuses primarily on the analysis of OA mass and composition data obtained from an Aerodyne Research Inc. compact time-of-flight aerosol mass spectrometer (C-ToF-AMS; *Drewnick et al., 2005; Canagaratna et al., 2007*). The AMS provides highly time-resolved mass concentrations of sub-micron, non-refractory aerosol, and a broad chemical characterisation across a complete range of constituent ion mass-to-charge ratios (m/z). Operation of the AMS, including calibration and necessary correction factors, during aircraft deployment (*Bahreini et al., 2003*) and specifically onboard the BAe-146 (*Crosier et al., 2007; Morgan et al., 2009; Taylor et al., 2014*) have been described in detail. Refractory black carbon (BC) was measured using a Droplet Measurement Technologies single particle soot photometer (SP-2; *Schwarz et al., 2006; Taylor et al., 2014*). Although analysis of the chemical and optical properties of single BC particles was not performed as part of this study, mass concentrations in smoke plumes, particularly in relation

126 to OA concentrations, were used as a means of evaluating the proportional contributions of different
127 combustion phases. A range of gas phase measurements were undertaken on the BAe-146, including
128 species used as tracers for both primary emissions and photochemical processing. CO mixing ratios
129 were measured with an Aerolaser AL5002 UV fluorescence analyser and O_3 by a Thermo Scientific
130 TEi49C UV photometric analyser as part of the standard complement of instrumentation for BAe-146
131 science flights. Additional instrumentation included a chemical ionisation mass spectrometer (CIMS;
132 *Nowak et al., 2007; Le Breton et al., 2012*) providing real-time measurements of HCN, which is
133 widely used as a tracer for BB emissions given that vegetation fires constitute its primary global
134 source (*Li et al., 2000; Sinha et al., 2003; Yokelson et al., 2007*). NO_x ($NO + NO_2$) and NO_y (NO_x
135 oxidation products, including HNO_3 and N_2O_5) act as important tracers for oxidation in aging plumes,
136 and were measured respectively by an Air Quality Design Inc. chemiluminescence NO_x analyser and
137 by thermal dissociation-laser induced fluorescence (TD-LIF; *Di Carlo et al., 2013*). The assembly of
138 gas phase measurements used within this analysis was completed by CO_2 mixing ratios from a Los
139 Gatos Research Inc. cavity enhanced absorption spectrometer-based fast greenhouse gas analyser
140 (FGGA; *O'Shea et al., 2013$_b$*). Aerosol size distributions in the range 20-350 nm were obtained from
141 a scanning mobility particle sizer (SMPS), with integrated distributions over this size range used as an
142 approximation of particle number concentration.
143
144 2.2 Data selection

145 Measurements from 5 BORTAS flights (B621-B624 and B626) were included in this
146 analysis. Flight B626 provided the only measurements of fresh BB plumes throughout the campaign,
147 with all other flights sampling air masses downwind of the source region at ages of several days. Data
148 were screened in order to isolate emissions with a biomass burning influence, resulting in a total
149 number of 26 valid plume interceptions (3 fresh and 23 aged) across the 5 flights. Screening was
150 performed using the guidelines proposed by *Capes et al.* (*2008*) and *Jolleys et al.* (*2012*) based upon
151 minimum $\triangle$CO (the excess CO concentration above background levels) and absolute number
152 concentrations. Respective thresholds of 20 ppb and 2000 cm^{-3} were applied for $\triangle$CO and number

concentration. Background concentrations for CO and other species were calculated for each flight according to minimum observed concentrations, which were applied to all measurements throughout the full vertical extent of sampling, given the limited variation in background concentrations with altitude. CO_2 was the only exception, with high variability both in and out of plume making it difficult to define an appropriate background concentration. As a result, only absolute concentrations are reported for CO_2, as opposed to excess values. A threshold of 0.003 was used for f_{60}, representing the ratio of levoglucosan-like species, which correspond to the *m/z* 60 peak in the AMS mass spectra (*Schneider et al., 2006; Alfarra et al., 2007*), to the total OA mass. This threshold is based upon observed background levels of f_{60} in OA emissions from urban and biogenic sources where BB influences are absent (*Cubison et al., 2011; Aiken et al., 2009; DeCarlo et al., 2008*). Levoglucosan and other anhydrous sugars such as mannosan and galactosan have been shown to be strongly associated with primary BB emissions (*Simoneit et al., 1999; Iinuma et al., 2007; Sullivan et al., 2008; Lee et al., 2010*). All data were also averaged to the temporal resolution of the AMS (~8 second time step on average) to enable direct comparison of different species.

Alternative screening procedures for BB influences have been applied throughout separate analyses of BORTAS data (*Palmer et al., 2013*). Concentrations of trace gases primarily produced by fire sources, including HCN and CH_3CN, are commonly used as indicators for BB plumes (*Li et al., 2000; Yokelson et al., 2007; Crounse et al., 2009; Yokelson et al., 2009; Akagi et al., 2011*). A scheme using a HCN concentration threshold of six times the standard deviation (6σ) has been used during BORTAS in an analysis of high sensitivity 1Hz chemical ionisation mass spectrometer (CIMS) measurements and their consistency with CO and CH_3CN concentrations (*Le Breton et al., 2013*). However, as many previous datasets do not include HCN measurementsa screening procedure using only OA, CO and number concentration data has been applied here, so that the approach can be used consistently across a broader range of data. This approach performs well when compared to the *Le Breton et al*. method, producing similarly strong correlations between HCN and CO for flights B621, B622, B624 and B626 (R^2 = 0.64, 0.52, 0.84 and 0.93) as the 6σ technique (R^2 = 0.83, 0.46, 0.82 and 0.81). HCN was not measured during B623, preventing comparison of classification schemes for this flight. Several flights carried out later in the campaign (B628-B630) also measured

181 highly aged plumes with a photochemical age of up to 11 days (*Palmer et al., 2013*). However,
182 correlations between △OA and △CO throughout these flights were exceptionally weak, yielding R^2
183 values consistently well below 0.1, contrasting with values in the range 0.39-0.74 for flights B621-
184 B624 and B626. These weak correlations from later flights suggest that sampled air masses lack a
185 common emission source and instead represent extensive mixtures of different plumes following
186 dispersion, or that emissions have been differentially processed to the extent that representative
187 properties can no longer be distinguished. As a result, data from these flights were omitted from this
188 analysis.

189 Throughout this study, extensive use is made of normalised measurements as a means of
190 assessing the relative abundances of different species. Normalising to a co-emitted, non-reactive
191 tracer such as △CO provides an emission ratio (ER) when calculated at source. Normalised excess
192 mixing ratios (NEMR) are used to represent these values for any other point in a plume away from
193 source along a Lagrangian trajectory, and account for the effects of dispersion as concentrations in
194 plumes decrease through dilution. These ratios can also be used as a marker for potential SOA
195 formation, as the longer atmospheric lifetime of CO (~1 month) relative to that of OA (on the order of
196 several weeks) makes it likely that any enhancement of the ratio between the two species will be a
197 result of the addition of OA, rather than increased removal of CO in isolation.

198

199 # 3. Results and discussion

200 ## 3.1 Spatial and temporal variability in BB emissions properties

201 Measurements of OA in BB plumes during the BORTAS flights included within this analysis
202 encompassed a wide range of ages, from at the source to up to 5 days after emission. The extent of
203 this diversity in age contributed to a high level of variability in plume properties, both across separate
204 research flights and between individual plumes encountered in different periods of the same flight.
205 Excess OA concentrations measured in-plume ranged from close to zero to around 180 μg m^{-3}, with
206 maximum △CO concentrations approaching 1000 ppb. Vertical profiles of both species are shown in
207 Figure 3, revealing an overall increase in concentrations throughout the boundary layer to a peak at

around 2000 m, before declining to background levels through the free troposphere. Significant elevations in both △OA and △CO occurred close to ground level, most likely as a result of influence from local sources. The observed decrease in concentration with altitude is more marked for △OA, which returns to background levels by 6000 m. Variability in △CO is much greater than △OA at higher altitudes. △CO concentrations of up to 800 ppb were observed between 5000–8000 m, whereas △OA did not exceed 30 μg m^{-3}. This disparity is attributed to the removal of OA from plumes encountered during flight B622 (20th July) by precipitation prior to sampling following advection through clouds, as corroborated by meteorological observations and back trajectory models (*Griffin et al., 2013; Taylor et al., 2014*). Wet deposition of aerosol reduced △OA to background levels, while △CO concentrations remained elevated to similar levels as observed at lower altitudes. Despite their biomass burning origin, the absence of OA and BC from these plumes resulted in their omission from this analysis.

The change in combustion conditions between different periods of BORTAS is reflected in the contrast between loadings of particulate and gas-phase species. Concentrations of the majority of sampled species in aged plumes during flights B621-B624, including OA, CO, CO_2 and BC, consistently exceeded those at source from B626, irrespective of the effect of dilution as plumes dispersed into the ambient atmosphere. During flight B626, △OA peaked at around 50 μg m^{-3}, with concentrations in more aged plumes exceeding this level by a factor of 3.6. △CO concentrations were also significantly elevated in aged plumes relative to fresh emissions. The contrast in properties between plumes of different ages is likely to be primarily affected by a change in the size and intensity of fires, rather than combustion phase alone, given the stronger association of both OA and CO production with predominantly smouldering combustion in the latter stages of fire evolution (*Reid et al., 2005*).

While the higher concentrations identified in aged plumes may be influenced to some extent by contributions from SOA, initial indications from calculated △OA/△CO ratios suggest this contribution did not provide any net increase in OA loadings. Figure 4 shows △OA/△CO for all 5 analyzed BORTAS flights, with average values determined from the gradient of linear least squares

235 regressions. Using this approach reveals that the average △OA/△CO close to source (0.190 ± 0.010,
236 where uncertainty represents the standard deviation in the fit) exceeds that for aged plumes (0.097 ±
237 0.002) by around 50%, with an overall campaign average of 0.104 ± 0.003. Average ratios for
238 individual flights sampling aged emissions range from 0.056 ± 0.003 (B624) to 0.114 ± 0.003 (B622),
239 giving an overall range of 0.058. The level of average △OA/△CO for fresh emissions from boreal
240 forest fires during BORTAS falls between the upper extent derived from the eucalypt forests of
241 northern Australia during ACTIVE (0.329), and lower ratios from several other campaigns where OA
242 enhancements were comparatively reduced (0.019-0.065; *Jolleys et al., 2012*). Average △OA/△CO
243 from aged plumes during BORTAS was again within the range identified from previous field
244 observations, although with closer proximity to ratios from the lower extent of the observed range,
245 including aged boreal forest fire plumes sampled during the Arctic Research of the Composition of
246 the Troposphere from Aircraft and Satellites (ARCTAS) campaign (*Hecobian et al., 2011*). The
247 extent of variability amongst aged emissions during ACTIVE also exceeded that observed during
248 BORTAS, with flights throughout the former campaign sampling plumes from fires in a number of
249 different source regions. However, analysis of ERs from vegetation fires performed under laboratory
250 conditions during the second Fire Lab At Missoula Experiment (FLAME II) also revealed extensive
251 variability in △OA/△CO directly at source, even amongst single plant species (*Jolleys et al., 2013*).
252 The single source region from which BORTAS plumes originated could therefore still be expected to
253 give rise to significantly contrasting △OA/△CO, while the effects of atmospheric processing during
254 transportation provide further perturbation of initial ERs. Flight-average △OA/△CO decreased
255 progressively for aged emissions as the distance from source at which plumes were intercepted
256 increased, with B622 performing a transit between Halifax and Quebec City, and B624 primarily
257 sampling plumes over the North Atlantic off the eastern coast of Nova Scotia and Newfoundland,
258 suggestive of OA losses during aging in these plumes from predominantly flaming sources.
259
260 3.2 Tracers for combustion conditions

While the evolution of △OA/△CO in aging plumes would appear to be strongly influenced by the effects of atmospheric processing, source conditions remain a critical factor in controlling OA production. Contrasts in △OA/△CO between fresh and aged OA are accompanied by varying properties with respect to the location and composition of plumes. Proportional contributions of OA mass fragment marker species differ between near and far-field measurements. f_{60} represents the prevalence of primary combustion products such as levoglucosan and is used as an indicator for fresh BB emissions (*Schneider et al., 2006; Alfarra et al., 2007*). Conversely, f_{44} is associated with the CO_2^+ ion derived from more aged OA as hydrocarbon fragments are oxidised to form organic acids (*Zhang et al., 2005; Aiken et al., 2008*), although *m/z* 44 is also a constituent of fresh smoke and has been shown to be significantly elevated at source, dependent on combustion conditions (*Weimer et al., 2008; Jolleys et al., 2013*). While strongly associated with saturated hydrocarbon fragments, *m/z* 43 can also originate from oxidised compounds such as aldehydes and ketones (*Alfarra et al., 2004*). Large contributions of *m/z* 43 have been observed within the mass spectra of OA during the laboratory combustion of a range of biomass fuels, typically accounting for a greater proportion of total OA mass than any other detected fragments (*Schneider et al., 2006*). This dominance of *m/z* 43 above *m/z* 44 amongst even compounds with high oxygen contents suggests the former can be produced preferentially during the fragmentation of oxygenated molecules, and as such f_{43} may prove to be an appropriate indictor of OA oxygenation at source.

Variations in the average proportions of *m/z* 43, 44 and 60 in OA between fresh and aged plumes are widely observed throughout BORTAS, emphasising the contrasting properties of aerosol of different ages. Mean f_{44} for B626, which comprised the only measurements of fresh OA during BORTAS, was lower than all other flights at 0.086 ± 0.014, with mean values for B621-B624 ranging from 0.104 to 0.139. This trend between the near and far-field is consistent with observations of boreal forest fire plumes during ARCTAS, where f_{44} was shown to increase as a function of plume transport time (*Cubison et al., 2011; Hecobian et al., 2011*). f_{60} was also shown to decrease concurrently with increasing f_{44} during ARCTAS, as a result of the oxidation of primary levoglucosan-type species with aging. However, mean f_{60} for BORTAS flight B626 was also amongst the lowest

288 throughout the campaign at 0.007 ± 0.004. Averages were higher for B621-B623 (0.010-0.017),
289 although B624 provided the lowest f_{60} with a mean of 0.005 ± 0.001.

290 While the higher mean f_{44} observed in the far-field is likely to primarily result from more
291 extensive oxidation of OA after longer periods of aging, the transition to more smouldering-
292 dominated combustion prior to sampling of near-field plumes could also have influenced observed
293 changes in composition. Elevated levels of f_{60} in aged plumes are indicative of such an effect, as *m/z*
294 60 would be expected to constitute a greater proportion of fresh OA, given its typical progressive
295 depletion through oxidation (*Cubison et al., 2011*). However, the relationships between f_{44}, f_{60} and
296 combustion phase are known to be complex and subject to considerable uncertainty. *Weimer et al.*
297 (*2008*) showed f_{60} to be more strongly associated with the initial flaming phase of combustion in wood
298 burners used for domestic heating, while f_{44} was higher during the later stages of the burning process
299 when smouldering combustion dominated. These trends are attributed to changes in combustion
300 behaviour and the consumption of different fuel components at each stage of the fire. In contrast, *Gao*
301 *et al.* (*2003*) reported significantly elevated levoglucosan concentrations from smouldering fires in
302 southern Africa, and severe depletion in emissions from flaming fires. Furthermore, *Lee et al.* (*2010*)
303 reported overall similarity in f_{60} across flaming and smouldering phases for open biomass fires carried
304 out in a laboratory setting as part of FLAME II, while the ratio of levoglucosan to total organic carbon
305 in filter samples from the same experiment shows a dependence on the fuel component burned
306 (*Sullivan et al., 2008*). Although both f_{44} and f_{60} were more frequently at a maximum during flaming
307 combustion in FLAME II burns (*Jolleys et al., 2013*), differences between phases were more
308 pronounced for f_{44}, with less variation amongst f_{60}. This behaviour is expected to result from greater
309 fire intensity during flaming combustion, although the specific effects of increased intensity on OA
310 composition through changing oxygen availability remain unclear.

311 Further indication of a shift in combustion phase is provided by the differences in f_{43} between
312 fresh and aged plumes, for which respective mean values were 0.123 ± 0.013 and 0.088 ± 0.012. The
313 low f_{44} and f_{60} for fresh OA suggest a dominance of smouldering fires, in agreement with the trends
314 identified by *Jolleys et al.* (*2013*). Additional variations in plume properties appear to substantiate an

association between f_{43} and smouldering combustion, including the correlation between periods of high f_{43} (>0.1) and low △BC /△OA (<0.02) in both fresh and aged plumes, with production of BC expected to be at a maximum during flaming combustion (*Reid & Hobbs, 1998*). Absence of a prominent flaming phase close to source is also corroborated by very low BC mass loadings, and reduced △BC /△OA relative to aged emissions, while the elevated △OA/△CO from these fires is consistent with the enhanced OA production typical of smouldering combustion (*Yokelson et al., 1997*). The lower △OA/△CO and f_{43}, but higher f_{44} and f_{60}, for aged OA would therefore be expected to derive from more intense, flaming-dominated combustion, which would also account for the significantly higher concentrations observed for △OA, △BC, △CO and △HCN despite plumes being progressively diluted over several days.

3.3 Effects of combustion conditions on vertical distributions

Altitudinal variations in plume composition further emphasise the importance of combustion conditions as a control on BB emissions and their propagation within the atmosphere. Profiles of aged plumes during BORTAS shown in Figure 5 highlight the shift in properties between the upper and lower troposphere, with higher altitude plumes more typical of flaming combustion. The △BC/△OA ratio is used as an indicator for the comparative contributions from flaming and smouldering combustion phases to the overall BB particulate loading (e.g. *Grieshop et al., 2009*), and is shown to increase through successive 500 m bins from 0.015 ± 0.003 at 500 m to 0.110 ± 0.055 at 6000 m, with the interquartile range increasing from 0.006 (2000 m) to 0.068 (5500 m). In contrast, △OA/△CO decreases over the same range, revealing the stark contrasts in plume composition at different altitudes and the apparent influence of fire properties at source. Mean △OA/△CO stands at 0.155 ± 0.061 and 0.196 ± 0.103 for the two bins closest to the surface, declining to 0.038 ± 0.015 at 6000 m. The interquartile range also decreases from 0.147 to 0.044 between 1500 and 5500 m, reflecting an overall reduction in variability with altitude.

With the exception of a few isolated points, △BC/△OA only rises above 0.02 in higher plumes where f_{43} is below 0.09, and remains consistently low when f_{43} is above this level

(Figure 6). This trend is in part due to the greater production of BC under flaming conditions, as reflected by corresponding distributions of high BC mass concentration, f_{60} and CO_2 (Figure 6a-c). Conversely, plumes sampled at lower altitudes exhibit characteristics more strongly associated with smouldering combustion (Figure 6d), and are comparable to fresh plumes with regards to low levels of $\triangle BC/\triangle OA$ and f_{60}, and high f_{43}. Weaker convection resulting from smouldering fires limits vertical transportation, retaining plumes within the boundary layer (*Andreae et al., 1996; Warneke et al., 2006; Burling et al., 2011*). The presence of flaming-derived emissions at higher altitudes alludes to an elevated injection height resulting from increased buoyancy and pyroconvection (*Fromm et al., 2005; Damoah et al., 2006*) driven by more intense fires earlier in the BORTAS campaign period (Figure 2). A similar dependence on combustion phase has previously been observed for the altitudinal distribution of different combustion products from boreal forest fires during ARCTAS (*Kondo et al., 2011*).

The altitudinal trends identified for $\triangle OA/\triangle CO$ and $\triangle BC/\triangle OA$ also show broad agreement with those of f_{43} and f_{60} respectively, with mean values for the former decreasing from 0.128 ± 0.006 to 0.078 ± 0.003 and latter increasing from 0.005 ± 0.001 to 0.015 ± 0.002. The directly opposing profiles of f_{43} and CO_2 (Figure 5c-d), along with the correlation of increased f_{60} with CO_2 and BC mass at high altitudes (Figure 7h-i), further underline the importance of initial combustion conditions for aged emissions. Minimum CO_2 concentrations within aged plumes were around 375 ppm, representing a minimal elevation above typical background levels for boreal Canadian forest environments (*Vay et al., 2011, Higuchi et al., 2003*). Although the distribution of CO_2 clearly reflects the influence of the biosphere closer to the surface through uptake in photosynthesis, expected source profiles also appear to be largely conserved, further corroborated by the sustained correlation between periods of high f_{43} and low CO_2, and vice versa, relative to levels throughout the rest of the aged plumes.

3.4 Aging as a driver for plume variability

Despite the apparent influence of combustion conditions on the vertical distribution and composition of aged emissions, the effects of transformations associated with atmospheric processing cannot be entirely discounted. Certain contrasting properties between emissions of different ages could also be less dependent on source conditions and more strongly influenced by processing throughout plume evolution. Differences between fresh and aged plumes in the respective relationships of total △OA loadings, and those normalised to △CO, with a number of tracers highlight the combined effects of source conditions and processing, and their changing influence with aging. Both △OA and △CO concentrations show a negative correlation with f_{44} (e.g. Figure 7a-b) and positive correlation with f_{60} (e.g. Figure 7f-g). Furthermore, when binning concentrations by f_{44}, maximum binned △OA and △CO both coincide with minimum f_{44} and vice versa. These overriding trends remain consistent for emissions of all ages, although the nature of the relationship changes in each case. Linear relationships appear consistently for △OA (R^2 = 0.51 and 0.80 with f_{44} and f_{60} respectively) and △CO (R^2 = 0.23 and 0.49) in fresh emissions. The same relationships also persist to an extent for △OA/△CO in fresh plumes (R^2 = 0.42 and 0.47). However, at a greater distance from source, correlations for △OA and △CO are consistently below 0.3, while there is no relationship between △OA/△CO and either f_{44} or f_{60}.

In addition to providing a tracer for source profiles in aged BB emissions, △BC/△OA can also be used as an indicator for OA processing. Observations of increasing △BC/△OA with aging have previously been attributed to the loss of OA mass through evaporation (*Liousse et al., 1995*). Similar behaviour has also been proposed as a possible cause of the overall reduction in △OA/△CO between BB plumes in the near and far-field throughout several campaigns across different global regions (*Jolleys et al., 2012*). Any decrease in △BC/△OA could therefore be considered a product, to a certain degree, of the addition of secondary organic mass from either the processing of BBOA or external sources. Measurements performed at lower altitudes (<2000 m) during flights B621 and B622 provide possible evidence to support such an effect. Both BC mass and f_{60} remain low during these periods, at less than 0.5 μg m^{-3} and 0.01 respectively, consistent with wider observations of smouldering fire emissions at low altitude during BORTAS. However, △CO concentrations are also

diminished and consistently below 100 ppb, relative to an average of 200 ppb for aged plumes, while △OA concentrations are comparable to levels in higher altitude, flaming-type plumes (~20 μg m^{-3}). These trends, which diverge from the expected characteristics for emissions of this origin, are further compounded by high $\triangle O_3/\triangle CO$ (>0.2), indicative of an elevated level of oxygenation and photochemical activity (*Mason et al., 2001; Parrington et al., 2013*). Formation of SOA from biogenic precursors has previously been observed in the forests of Ontario (*Slowik et al., 2010*). These SOA events were also characterised by △OA/△CO levels far in excess of those derived for BB emissions during the same study. In accordance with this trend, △OA/△CO within the low altitude plumes in B621 and B622 were consistently above the average for aged emissions (0.097), reaching as high as ~0.4. There is subsequently considerable evidence to support biogenic SOA as a potential contributor to the OA burden during BORTAS, which could provide further enhancement of △OA/△CO as demonstrated by the *Slowik et al.* (*2010*) Ontario study. Whilst the further properties of aged plumes discussed here would suggest this effect is isolated and limited in its overall impact, it presents a further source of uncertainty for any attempts to develop parameterisations for the contribution of forest fires to regional and global OA budgets.

Although f_{60} displays a level of consistency with flaming combustion products in upper troposphere plumes during BORTAS, and increases on average with increasing altitude, further trends oppose the expected relationships for different combustion phases. Maximum concentrations of △OA, △BC, △CO and CO_2 all coincide with high f_{60} (0.025-0.300) and show a reduction as f_{60} decreases (Figure 7f-i). Overall correlations between each species and f_{60} are all positive, albeit with varying fit coefficients. R^2 values were highest for CO_2 and △BC (0.52 and 0.47), reflecting their stronger associations with flaming combustion (*Crutzen & Andreae, 1990; Reid et al., 2005*). Correlations with △OA and △CO were weaker (R^2 = 0.28 and 0.23), as would be expected given production of each is greatest during the smouldering phase (*Ferek et al., 1998; Andreae & Merlet; 2001; Gao et al., 2003*). While trends with $\triangle O_3/\triangle CO$ show f_{60} to decrease with aging (Figure 7j), the underlying relationships identified with all other species suggest f_{60} may prove to be a more resilient tracer for overall plume intensity rather than combustion conditions at long aging times.

However, *Petzold et al.* (*2007*) demonstrated export efficiencies of up to 90% for BC following intercontinental transport of boreal forest fire plumes. In the absence of significant removal through wet deposition, △BC/△CO in plumes encountered at altitudes above 4km remained consistent with typical source values, indicating that mixing of emissions can be suppressed where fire intensity is sufficient to generate elevated injection heights. Conversely, the weaker convection associated with smouldering combustion may lead to emissions being retained within the boundary layer, contributing to the typically higher levels of △OA/△CO and f_{43} at low altitudes.

3.5 Tracer evolution during BORTAS

The progression from f_{60} to f_{44} can provide a useful metric to assess the evolution of OA composition with aging. Figure 8 shows the nature of this progression for both fresh and aged OA, together with further trends with several additional parameters. A strong linear relationship (R^2 = 0.72) is identified for emissions close to source. However, these observations comprised measurements of three separate periods of flight B626, and reveal a clear discrepancy for one of these periods. Measurements performed further to the east of the source region, on a transect from approximately 52.3° N, 90.0° W to 52.8° N, 91.3° W (a 'downwind' plume) yielded higher f_{44} than any other fresh plumes, with f_{60} not exceeding 0.045. The two remaining sets of plumes ('source' plumes) were both encountered within a region where active fires were present at around 52.4-52.8° N, 93.0-93.7° W. Despite sampling taking place roughly two hours apart, and over a slightly different geographical extent, the f_{44}/f_{60} relationship remains highly consistent across all 'source' plumes, with an R^2 of 0.82. The higher levels of f_{44} and absence of a trend with f_{60} in the ‘downwind’ plume indicate OA is more heavily oxidised than in the fresher ‘source’ plumes. This contrast in oxygenation is linked to other changes between plumes, including apparent photochemical age, which in this instance is represented by the $-\log(NO_x/NO_y)$ ratio (*Kleinman et al., 2008; DeCarlo et al., 2008*). Levels of the ratio are significantly elevated in the 'downwind' plume from B626 (Figure 8f, left panel), with an average of 1.45 ± 0.43, exceeding the mean value of 1.09 ± 0.29 for highly aged plumes sampled during flights B621-B624. CO_2 concentrations during this period are also higher than

for the remainder of B626 (Figure 8b, left panel), with an average of 378.6 ± 0.6 ppm compared to 375.0 ± 1.3 ppm closer to source. The $-\log(NO_x/NO_y)$ photochemical clock is also shown to increase throughout 'source' plumes, with f_{44} and f_{60} changing in a manner consistent with the increasing oxidation of OA, and is further corroborated by a trend of increasing $\triangle O_3/\triangle CO$ (Figure 8e, left panel). However, these changes also coincide with a trend of decreasing $\triangle OA/\triangle CO$ (Figure 8c, left panel), belying the expected addition of OA mass resulting from increasing oxygenation as semivolatile products condense to the particle phase. Average $\triangle OA/\triangle CO$ is similar for the two 'source' plumes (0.165 ± 0.042 and 0.180 ± 0.045), but is lower in the more photochemically aged 'downwind' plume (0.114 ± 0.015). It is difficult to speculate on the significance of any link between a higher rate of oxidation and an overall reduction in $\triangle OA/\triangle CO$ given the continuing uncertainty regarding the processes affecting OA in aging BB plumes. *Yokelson et al.* (*2009*) reported that $\triangle OA/\triangle CO$ increased by a factor of 2.3 over a period of 1.4 hours for plumes from fires in the Yucatan region of Mexico, coinciding with a comparably high f_{44}/f_{60} gradient to that in the 'downwind' section of B626. Conversely, an increase in f_{44} has also been shown in conjunction with stable or even decreasing levels of $\triangle OA/\triangle CO$ (*Capes et al., 2008; Cubison et al., 2011; Akagi et al., 2012; Jolleys et al., 2012*), suggesting OA loss through evaporation has an equally important effect throughout plume evolution.

Linear relationships between f_{44} and f_{60} are weaker for more aged plumes sampled at a greater distance downwind, with an overall R^2 value for all plumes of 0.44 and individual flights ranging from 0.01 (B624) to 0.32 (B622). The overall decline of f_{60} again appears to be strongly influenced by distance from the source region and the physical age of plumes, decreasing from a maximum of ~0.027 in B622 to a minimum of ~0.004 in B624. An effect of dilution is evident, given the concurrent reduction in both $\triangle CO$ and CO_2 with decreasing f_{60} and increasing f_{44} (Figure 8a-b, right panels). $\triangle O_3/\triangle CO$ shows the reverse progression, increasing with the oxygenation of OA (Figure 8e, right panel), while $-\log(NO_x/NO_y)$ does not exhibit the strong trend observed for near-field measurements but is typically higher and reflects longer aging times (Figure 8f). However, $-\log(NO_x/NO_y)$ ratios were highest on average for the 'downwind' plume in B626, which did not

provide any significant indication of net addition of OA mass. While the highest average △OA/△CO ratio for an individual plume throughout the entirety of BORTAS was derived for one of the 'source' plumes during B626, two aged plumes from B622 exhibited average △OA/△CO of a similar magnitude (0.120 ± 0.080 and 0.119 ± 0.042), with each plume representing a different region of f_{44}/f_{60} space.

The contrasting behaviours of various tracers throughout fresh and aged plumes highlights the different ways in which these properties can be used to evaluate influences on BBOA evolution. With regards to f_{44}, the consistently higher values observed in aged plumes, and the strong trends identified with indicators of photochemical aging such as $-\log(NO_x/NO_y)$ and $\triangle O_3/\triangle CO$ close to source (Figure 8e-f, left panels), substantiate its use as a tracer for OA aging. Although f_{60} exhibits the same clear relationship with $-\log(NO_x/NO_y)$ and $\triangle O_3/\triangle CO$ in fresh plumes, albeit reversed and decreasing with aging, values are higher on average amongst aged plumes. Given the overall trend of increasing f_{44} with decreasing f_{60} remains for aged OA, the longer periods of aging to which these plumes have been exposed would be expected to bring about a more extensive reduction in the latter tracer. The elevation in f_{60} relative to fresh plumes would therefore seem to stem from the contrasting dominant combustion phases associated with plumes of different ages, and the persistence of high levels in flaming-derived OA at greater altitudes. In contrast, f_{43} shows an overall reduction with aging, with mean values of 0.123 ± 0.013 and 0.088 ± 0.012 for near and far-field plumes respectively, consistent with the oxidation of primary OA components over time. However, overall trends with $-\log(NO_x/NO_y)$ and $\triangle O_3/\triangle CO$ in fresh plumes are generally positive, albeit with fairly weak correlation coefficients (R^2 = 0.12 and 0.34), resulting in f_{43} peaking at greater photochemical ages. This relationship contradicts that which would be expected in aging OA (*Ng et al., 2010; Morgan et al., 2010*), and suggests additional factors may be contributing to the observed variability in f_{43}. However, fragmentation of oxygenated aldehyde and ketone molecules has been shown to produce elevated levels of f_{43} relative to f_{44} in BB emissions (*Schneider et al., 2006*), suggesting possible contributions from secondary formation. Values of f_{43} in fresh OA are almost entirely greater than 0.1, while this threshold is most frequently exceeded amongst aged OA in plumes below around

503 3000 m (Figure 5d). These lower altitude plumes exhibit the same low △BC/△OA levels as
504 identified close to source (< 0.02), in contrast to the greater range in △BC/△OA (up to 0.15)
505 coinciding with lower f_{43} (Figure 6). Differing distributions of f_{43} in aged plumes, and the prescribed
506 similarities with near-field observations, may reflect an influence of changing combustion conditions,
507 with f_{43} seemingly more prominent in OA from smouldering fires. As a result, f_{43} may prove to be a
508 more suitable tracer for source conditions rather than the effects of aging, although comparison
509 between different combustion phases at source would be required in order to fully constrain any such
510 relationship.
511
512 3.6 Campaign intercomparison and evaluation of f_{44} and f_{60} tracers

513 The progression of f_{44} and f_{60} throughout BORTAS shows a number of similarities with
514 observations from other field campaigns and laboratory experiments. Distributions for fresh and aged
515 emissions from BORTAS and montane forest fires during the Megacities Initiative: Local and Global
516 Research Observations (MILAGRO) campaign are presented in Figure 9, along with data from
517 numerous plumes measured during ARCTAS-B. Data are also shown for the combustion of boreal
518 forest plant species under laboratory conditions as part of FLAME II. Similar trends in f_{44}/f_{60} for fresh
519 and aged emissions are identified for BORTAS and MILAGRO, with average f_{44} increasing with
520 aging in both cases. A significant contrast is also evident in the distributions of f_{60}, which is higher on
521 average for fresh plumes in MILAGRO and aged plumes in BORTAS, possibly as a result of the
522 reduced intensity of fires sampled close to source. Average △OA/△CO is again lower for the aged
523 fraction in MILAGRO, decreasing from 0.051 ± 0.001 in fresh plumes to 0.041 ± 0.001 (*Jolleys et al.,*
524 *2012*), consistent with a loss of OA. The lower magnitude of these ratios is likely to be a consequence
525 of different fuel properties and resulting combustion conditions, as strongly-flaming grass fires are
526 expected to have made a significant contribution to smoke plumes sampled at the Paso de Cortes
527 measurement site (*Jolleys et al., 2013*). Figure 9 also emphasises the differences in emissions from
528 boreal forest fires during ARCTAS-B and BORTAS. Plumes encountered close to source in each
529 campaign exhibit contrasting levels of f_{60}, reflecting the dominance of different combustion phases in

each set of measurements. Unlike the heavily smouldering fires sampled in flight B626, the plume from a fire at Lake McKay in northwestern Saskatchewan was produced by highly intense, flaming fires (*Cubison et al., 2011*). The Lake McKay fires subsequently yielded higher f_{60} than was observed for any BORTAS plumes, peaking at around 0.05. As the Lake McKay plume was tracked downwind, f_{44} increased to ~0.12, comparable to the upper extent for fresh plumes in BORTAS. Although f_{60} decreased to ~0.015, this level remained above the majority of the distribution from BORTAS. Similarly high levels of f_{60} were observed for black spruce fires during FLAME II. However, f_{44} from these burns was generally exceptionally low, as would be expected given the direct measurement at source and lack of aging. Higher f_{44} comparable to the range identified in ambient emissions did occur in chamber fires for plant species representing environments other than boreal forests, with average values particularly high for chaparral fuels. Montane forest fuels, which like the boreal equivalent comprised samples of coniferous species, also yielded f_{44} up to ~0.15, although such fires largely involved drier, woody plant material leading to more flaming-dominated combustion (*Jolleys et al., 2013*).

The different f_{44} and f_{60} regimes in ambient and chamber fires, and their conflicting relationships with combustion phases, suggest their use as tracers for processing of BBOA is highly dependent on both fire properties and experimental conditions. Throughout FLAME II, f_{44} was shown to be more strongly associated with flaming combustion, as increased intensity and turbulent mixing enhanced the supply of oxygen to fires. In contrast, the rapid increase in f_{44} in fresh OA from smouldering fires during BORTAS, to levels comparable to more extensively aged plumes, indicate that f_{44} is strongly influenced by post-emission processing under ambient conditions. Relationships with f_{60} are more consistent, being higher on average more frequently for flaming-dominated fires under laboratory conditions, and showing a stronger association with seemingly flaming-derived aged emissions during BORTAS. Probability density functions (PDFs) for f_{44} and f_{60} in fresh and aged emissions from BORTAS, along with source emissions from fires involving boreal and montane forest fuels during FLAME II, are shown in Figure 10. The clear separation in f_{44} distributions between chamber and ambient measurements reflects the role of aging in determining the level of

557 oxidation in BBOA, as further evidenced by the enhancement in plumes in the far-field above those at
558 source. However, the trend of increasing f_{44} in fresh plumes suggests that this processing can occur
559 over very short timescales under certain atmospheric conditions. Rapid oxidation of BB smoke
560 plumes has previously been inferred from the addition of secondary OA mass within ~1 hour of
561 emission (*Gao et al., 2003; Yokelson et al., 2009*), corroborating the BORTAS trend. Values of f_{44}
562 coinciding with peak concentrations for a number of combustion products are also shown in Figure
563 10. These peak concentrations show a good agreement with prescribed combustion phase
564 relationships for FLAME II data, with $\triangle CO_2$ reaching a maximum when f_{44} is higher, and hence
565 combustion more flaming-dominated, while $\triangle$OA and $\triangle$CO peak at a lower f_{44}. The same trends are
566 also observed throughout BORTAS, with peak concentrations for $\triangle CO_2$ and $\triangle$BC coinciding with
567 higher levels of f_{44} than those of $\triangle$CO or $\triangle$OA. PDFs for f_{60} exhibit the same trend amongst ambient
568 plumes, shifting to higher values with aging. Distributions are also broadened for emissions from
569 chamber burns, for which levoglucosan-type species constitute a larger proportion of the total OA
570 mass. The very low peak for near-field BORTAS plumes could be influenced by both the absence of
571 a significant flaming phase and subsequent oxidation of primary OA (*Cubison et al., 2011*),
572 contributing to the increase in f_{44}. The variable gradients for f_{44}/f_{60} regressions (Figure 9) indicate a
573 slower rate of decay for levoglucosan-type OA in aged BORTAS plumes compared to their
574 equivalents from MILAGRO. Furthermore, mean f_{60} in aged MILAGRO plumes (0.006 ± 0.003) was
575 lower than in fresh plumes (0.018 ± 0.006), while the opposite was true for BORTAS plumes (0.012 ±
576 0.005 and 0.007 ± 0.004 respectively). As such, the slower decline of f_{60} and potential influences
577 from more strongly flaming combustion may contribute towards the observed enhancement in aged
578 BORTAS plumes, while a faster rate of oxidation and largely smouldering fires reduce levels closer to
579 source.
580

581 ## 4. Conclusions

582 Smoke plumes from Canadian boreal forest fires have been shown to exhibit highly variable
583 properties over a range of ages and combustion phases. Average $\triangle$OA/$\triangle$CO in 3 plumes sampled

584 close to source (0.190 ± 0.010) exceed ratios in the far-field from 23 interceptions (0.056 ± 0.003 to
585 0.114 ± 0.003), reaffirming an absence of significant net SOA formation for aging BB emissions, at
586 least to an extent that provides an elevation above initial OA production at source. While contrasting
587 aging behaviours and significant SOA formation have been identified in some studies, an absence of
588 increasing △OA/△CO has been observed in several previous BB assessments. The trend of
589 decreasing △OA/△CO with increasing distance from source in BORTAS further emphasises the
590 importance of source conditions for aging plumes. High levels of typical flaming combustion
591 products were identified in highly aged plumes following transportation over a period of several days.
592 Enhancements in △BC/△OA and f_{60} were most prominent within the free troposphere, typically
593 displaying an overall increase with altitude, while aged OA sampled within the boundary layer
594 showed stronger evidence for production by smouldering combustion.

595 Aging of BBOA during BORTAS has been extensively evaluated using the key tracers f_{44} and
596 f_{60} from the AMS mass spectrum. An enhancement in f_{44} was determined for far-field plumes, where
597 the mean value of 0.121 ± 0.016 significantly exceeded that in the near-field (0.086 ± 0.014).
598 Similarly, f_{60} remained higher in aged plumes (0.012 ± 0.005) than those close to source (0.007 ±
599 0.004), in spite of the concurrent increase in oxygenation and expected processing of primary OA
600 components. These trends highlight the importance of both source conditions and processing for OA
601 composition in BB plumes. While the influence of combustion phase on f_{44} remains highly uncertain
602 given contrasting relationships with smouldering and flaming combustion reported in different
603 studies, increases observed close to source suggest oxidation can occur over very short timescales
604 after emission. This rapid processing is further corroborated by concurrent increases in
605 photochemical tracers such as $\triangle O_3/\triangle CO$ and $-\log(NO_x/NO_y)$ ratios in plumes sampled near to
606 source. The increasing oxygenation of BBOA is not accompanied by an increase in △OA/△CO,
607 which shows no significant change with $\triangle O_3/\triangle CO$ and decreases on average with $-\log(NO_x/NO_y)$
608 over short aging times. A lack of △OA/△CO enhancement irrespective of evidence for wider
609 transformations therefore further substantiates the impact of OA losses in these aging BB plumes.

Presenting the changing composition of BBOA in f_{44}/f_{60} space reveals a consistent progression from high f_{60} to high f_{44} as primary levoglucosan-like species are lost through oxidation. Similar transitions occur across multiple datasets encompassing smoke plumes of varying origins and ages, although the gradients and extents of distributions show some variability between campaigns. Levels of f_{44} are also comparatively depleted in chamber burns of boreal forest fuels. The absence of aging and a strong association with flaming combustion, and hence oxygen supply through entrainment, in these experiments denote alternative tracer functions under laboratory and ambient conditions. While f_{44} can act as an indicator for oxygenation through combustion processes in chamber experiments, the influence of aging is likely to limit such application for ambient emissions. However, f_{60} has been shown to act as a long-lived tracer for BB emissions, despite evidence for an overall reduction with increasing f_{44}.

Analysis of measurements performed during the BORTAS campaign has provided further insight to the variability associated with BB emissions and the processes affecting changes in BBOA loadings and composition over time. However, there remains considerable uncertainty regarding the main drivers of OA processing. While data from BORTAS provide evidence for the influence of a range of source and aging processes, the extents of any effects on aging BBOA are unclear, particularly with regard to their consistency across different environments and fire types. Key trends identified in this analysis, such as the comparatively lower levels of f_{60} close to source, contradict previous findings and highlight the lack of consistency prevalent amongst many aspects of investigations focusing on BB emissions. Further research specifically targeting these areas of uncertainty is therefore essential in order to understand the cause of these disparities and provide more reliable parameterisations of BB contributions to the atmospheric aerosol burden.

Acknowledgments

The authors would like to acknowledge financial support from the United Kingdom Natural Environment Research Council (NERC) under grant number NE/F017391/1, and thank all those involved in the BORTAS project. Airborne data was obtained

636 using the FAAM BAe-146 Atmospheric Research Aircraft (ARA) operated by Directflight Ltd (DFL)
637 and managed by the Facility for Airborne Atmospheric Measurements (FAAM), which is a joint
638 entity of NERC and the UK Meteorological Office. M. D. Jolleys was supported by a NERC
639 studentship NE/H525162/1. P. I. Palmer also acknowledges support from the Leverhulme Trust.

References

Aiken, A. C., et al. (2008), O/C and OM/OC ratios of primary, secondary, and ambient organic aerosols with high-resolution time-of-flight aerosol mass spectrometry, *Environmental Science & Technology*, *42*(12), 4478-4485, doi:10.1021/es703009q.

Aiken, A. C., et al. (2009), Mexico City aerosol analysis during MILAGRO using high resolution aerosol mass spectrometry at the urban supersite (T0) - Part 1: Fine particle composition and organic source apportionment, *Atmospheric Chemistry and Physics*, *9*(17), 6633-6653.

Akagi, S. K., R. J. Yokelson, C. Wiedinmyer, M. J. Alvarado, J. S. Reid, T. Karl, J. D. Crounse, and P. O. Wennberg (2011), Emission factors for open and domestic biomass burning for use in atmospheric models, *Atmospheric Chemistry and Physics*, *11*(9), 4039-4072, doi:10.5194/acp-11-4039-2011.

Akagi, S. K., et al. (2012), Evolution of trace gases and particles emitted by a chaparral fire in California, *Atmospheric Chemistry and Physics*, *12*(3), 1397-1421, doi:10.5194/acp-12-1397-2012.

Alfarra, M. R., H. Coe, J.D. Allan, K.N. Bower, H. Boudries, M.R. Canagaratna, J.L. Jimenez, J.T. Jayne, A.A. Garforth, S.M. Li, and D.R. Worsnop (2004), Characterization of urban and rural organic particulate in the Lower Fraser Valley using two Aerodyne Aerosol Mass Spectrometers, *Atmospheric Environment*, *38* (34), 5745-5758, doi: 10.1016/ j.atmosenv.2004.01.054.

Alfarra, M. R., A. S. H. Prevot, S. Szidat, J. Sandradewi, S. Weimer, V. A. Lanz, D. Schreiber, M. Mohr, and U. Baltensperger (2007), Identification of the mass spectral signature of organic aerosols from wood burning emissions, *Environmental Science & Technology*, *41*(16), 5770-5777, doi:10.1021/es062289b.

Andreae, M. O., E. Atlas, H. Cachier, W. R. Cofer III, G. W. Harris, G. Helas, R. Koppmann, J.-P. Lacaux and D. E. Ward (1996), Trace gas and aerosol emissions from savanna fires, in *Biomass Burning and Global Change*, edited by S. Levine, pp. 278-295, MIT Press, Cambridge, Mass.

Andreae, M. O., and P. Merlet (2001), Emission of trace gases and aerosols from biomass burning, *Global Biogeochemical Cycles*, *15*(4), 955-966.

Bahreini, R., J. L. Jimenez, J. Wang, R. C. Flagan, J. H. Seinfeld, J. T. Jayne, and D. R. Worsnop (2003), Aircraft-based aerosol size and composition measurements during ACE-Asia using an Aerodyne aerosol mass spectrometer, *Journal of Geophysical Research-Atmospheres*, *108*(D23), doi:10.1029/2002jd003226.

Bond, T. C., D. G. Streets, K. F. Yarber, S. M. Nelson, J. H. Woo, and Z. Klimont (2004), A technology-based global inventory of black and organic carbon emissions from combustion, *Journal of Geophysical Research-Atmospheres*, *109*(D14), doi:10.1029/2003jd003697.

Burling, I. R., R. J. Yokelson, S. K. Akagi, S. P. Urbanski, C. E. Wold, D. W. T. Griffith, T. J. Johnson, J. Reardon, and D. R. Weise (2011), Airborne and ground-based measurements of the trace gases and particles emitted by prescribed fires in the United States, *Atmospheric Chemistry and Physics*, *11*(23), 12197-12216, doi:10.5194/acp-11-12197-2011.

Canagaratna, M. R., et al. (2007), Chemical and microphysical characterization of ambient aerosols with the aerodyne aerosol mass spectrometer, *Mass Spectrometry Reviews*, *26*(2), 185-222, doi:10.1002/mas.20115.

Capes, G., B. Johnson, G. McFiggans, P. I. Williams, J. Haywood, and H. Coe (2008), Aging of biomass burning aerosols over West Africa: Aircraft measurements of chemical composition, microphysical properties, and emission ratios, *Journal of Geophysical Research-Atmospheres*, *113*(D20), doi:10.1029/2008jd009845.

Crosier, J., J. D. Allan, H. Coe, K. N. Bower, P. Formenti, and P. I. Williams (2007), Chemical composition of summertime aerosol in the Po Valley (Italy), northern Adriatic and Black Sea, *Quarterly Journal of the Royal Meteorological Society*, *133*, 61-75, doi:10.1002/qj.88.

Crounse, J. D., et al. (2009), Biomass burning and urban air pollution over the Central Mexican Plateau, *Atmospheric Chemistry and Physics*, *9*(14), 4929-4944.

Crutzen, P. J., and M. O. Andreae (1990), Biomass Burning in the Tropics - Impact on Atmospheric Chemistry and Biogeochemical Cycles, *Science*, *250*(4988), 1669-1678, doi:10.1126/science.250.4988.1669.

Cubison, M. J., et al. (2011), Effects of aging on organic aerosol from open biomass burning smoke in aircraft and laboratory studies, *Atmospheric Chemistry and Physics*, *11*(23), 12049-12064, doi:10.5194/acp-11-12049-2011.

Damoah, R., N. Spichtinger, R. Servranckx, M. Fromm, E. W. Eloranta, I. A. Razenkov, P. James, M. Shulski, C. Forster, and A. Stohl (2006), A case study of pyro-convection using transport model and remote sensing data, *Atmospheric Chemistry and Physics*, *6*, 173-185.

DeCarlo, P. F., et al. (2008), Fast airborne aerosol size and chemistry measurements above Mexico City and Central Mexico during the MILAGRO campaign, *Atmospheric Chemistry and Physics*, *8*(14), 4027-4048.

DeCarlo, P. F.; et al. (2010), Investigation of the sources and processing of organic aerosol over the Central Mexican Plateau from aircraft measurements during MILAGRO. *Atmospheric Chemistry and Physics, 10*(12), 5257-5280.

Di Carlo, P., et al. (2013), Aircraft based four-channel thermal dissociation laser induced fluorescence instrument for simultaneous measurements of NO2, total peroxy nitrate, total alkyl nitrate, and HNO3, *Atmospheric Measurement Techniques*, *6*(4), 971-980, doi:10.5194/amt-6-971-2013.

Drewnick, F., et al. (2005), A new time-of-flight aerosol mass spectrometer (TOF-AMS) - Instrument description and first field deployment, *Aerosol Science and Technology*, *39*(7), 637-658, doi:10.1080/02786820500182040.

Ferek, R. J., J. S. Reid, P. V. Hobbs, D. R. Blake, and C. Liousse (1998), Emission factors of hydrocarbons, halocarbons, trace gases and particles from biomass burning in Brazil, *Journal of Geophysical Research-Atmospheres*, *103*(D24), 32107-32118.

Forster, P., et al. (2007), Changes in Atmospheric Constituents and in Radiative Forcing, in: *Climate Change 2007: The Physical Science Basis, contribution of Working Group I to the Fourth Assessment Report of the Intergovernmental Panel on Climate Change*, edited by: Solomon, S. D., Qin, M., Manning, Z., Chen, M., Marquis, K. B., Averyt, M. T., and Miller, H. L., p. 129–234, Cambridge University Press, Cambridge, United Kingdom and New York, NY, USA.

Fromm, M., R. Bevilacqua, R. Servranckx, J. Rosen, J. P. Thayer, J. Herman, and D. Larko (2005), Pyro-cumulonimbus injection of smoke to the stratosphere: Observations and impact of a super

720 blowup in northwestern Canada on 3-4 August 1998, *Journal of Geophysical Research-Atmospheres*,
721 *110*(D8), doi:10.1029/2004jd005350.

722 Gao, S., D. A. Hegg, P. V. Hobbs, T. W. Kirchstetter, B. I. Magi, and M. Sadilek (2003), Water-
723 soluble organic components in aerosols associated with savanna fires in southern Africa:
724 Identification, evolution, and distribution, *Journal of Geophysical Research-Atmospheres*, *108*(D13),
725 doi:10.1029/2002jd002324.

726 Grieshop, A. P., J. M. Logue, N. M. Donahue, and A. L. Robinson (2009), Laboratory investigation of
727 photochemical oxidation of organic aerosol from wood fires 1: measurement and simulation of
728 organic aerosol evolution, *Atmospheric Chemistry and Physics*, *9*(4), 1263-1277.

729 Griffin, D., et al. (2013), Investigation of CO, C_2H_6 and aerosols in a boreal fire plume over eastern
730 Canada during BORTAS 2011 using ground- and satellite-based observations and model simulations,
731 *Atmospheric Chemistry and Physics*, *13*(20), 10227-10241.

732 Hallquist, M., et al. (2009), The formation, properties and impact of secondary organic aerosol:
733 current and emerging issues, *Atmospheric Chemistry and Physics*, *9*(14), 5155-5236.

734 Hecobian, A., et al. (2011), Comparison of chemical characteristics of 495 biomass burning plumes
735 intercepted by the NASA DC-8 aircraft during the ARCTAS/CARB-2008 field campaign,
736 *Atmospheric Chemistry and Physics*, *11*(24), 13325-13337, doi:10.5194/acp-11-13325-2011.

737 Hennigan, C. J., et al. (2011), Chemical and physical transformations of organic aerosol from the
738 photo-oxidation of open biomass burning emissions in an environmental chamber, *Atmospheric*
739 *Chemistry and Physics*, *11*(15), 7669-7686, doi:10.5194/acp-11-7669-2011.

740 Heringa, M. F., P. F. DeCarlo, R. Chirico, T. Tritscher, J. Dommen, E. Weingartner, R. Richter, G.
741 Wehrle, A. S. H. Prevot, and U. Baltensperger (2011), Investigations of primary and secondary
742 particulate matter of different wood combustion appliances with a high-resolution time-of-flight
743 aerosol mass spectrometer, *Atmospheric Chemistry and Physics*, *11*(12), 5945-5957, doi:10.5194/acp-
744 11-5945-2011.

745 Higuchi, K., D. Worthy, D. Chan, and A. Shashkov (2003), Regional source/sink impact on the
746 diurnal, seasonal and inter-annual variations in atmospheric CO2 at a boreal forest site in Canada,
747 *Tellus Series B-Chemical and Physical Meteorology*, *55*(2), 115-125, doi:10.1034/j.1600-
748 0889.2003.00062.x.

749 Iinuma, Y., E. Bruggemann, T. Gnauk, K. Muller, M. O. Andreae, G. Helas, R. Parmar, and H.
750 Herrmann (2007), Source characterization of biomass burning particles: The combustion of selected
751 European conifers, African hardwood, savanna grass, and German and Indonesian peat, *Journal of*
752 *Geophysical Research-Atmospheres*, *112*(D8), doi:10.1029/2006jd007120.

753 Jimenez, J. L., et al. (2009), Evolution of Organic Aerosols in the Atmosphere, *Science*, *326*(5959),
754 1525-1529, doi:10.1126/science.1180353.

755 Jolleys, M. D., et al. (2012), Characterizing the Aging of Biomass Burning Organic Aerosol by Use of
756 Mixing Ratios: A Meta-analysis of Four Regions, *Environmental Science & Technology*, *46*(24),
757 13093-13102, doi:10.1021/es302386v.

758 Jolleys, M. D., et al. (2013), Organic Aerosol Emission Ratios from the Laboratory Combustion of
759 Biomass Fuels, in preparation.

760 Kleinman, L. I., et al. (2008), The time evolution of aerosol composition over the Mexico City
761 plateau, *Atmospheric Chemistry and Physics*, *8*(6), 1559-1575.

762 Kondo, Y., et al. (2011), Emissions of black carbon, organic, and inorganic aerosols from biomass
763 burning in North America and Asia in 2008, *Journal of Geophysical Research-Atmospheres*, *116*,
764 doi:10.1029/2010jd015152.

765 Le Breton, M., et al. (2012), Airborne observations of formic acid using a chemical ionisation mass
766 spectrometer, *Atmospheric Measurement Techniques*, *5*(12), 3029-3039, doi: 10.5194/amt-5-3029-
767 2012.

768 Le Breton, M., et al. (2013), Airborne hydrogen cyanide measurements using a chemical ionisation
769 mass spectrometer for the plume identification of biomass burning forest fires, *Atmospheric*
770 *Chemistry and Physics Discussions*, *13*, 5649-5685, doi:10.5194/acpd-13-5649-2013.

771 Lee, T., et al. (2010), Chemical Smoke Marker Emissions During Flaming and Smoldering Phases of
772 Laboratory Open Burning of Wildland Fuels, *Aerosol Science and Technology*, *44*(9), I-V,
773 doi:10.1080/02786826.2010.499884.

774 Li, Q. B., D. J. Jacob, I. Bey, R. M. Yantosca, Y. J. Zhao, Y. Kondo, and J. Notholt (2000),
775 Atmospheric hydrogen cyanide (HCN): Biomass burning source, ocean sink?, *Geophysical Research*
776 *Letters*, *27*(3), 357-360, doi:10.1029/1999gl010935.

777 Liousse, C., C. Devaux, F. Dulac, and H. Cachier (1995), Aging of Savanna Biomass Burning
778 Aerosols - Consequences on their Optical Properties, *Journal of Atmospheric Chemistry*, *22*(1-2), 1-
779 17, doi:10.1007/bf00708178.

780 Mason, S. A., R. J. Field, R. J. Yokelson, M. A. Kochivar, M. R. Tinsley, D. E. Ward, and W. M. Hao
781 (2001), Complex effects arising in smoke plume simulations due to inclusion of direct emissions of
782 oxygenated organic species from biomass combustion, *Journal of Geophysical Research-*
783 *Atmospheres*, *106*(D12), 12527-12539.

784 McMeeking, G. R., et al. (2009), Emissions of trace gases and aerosols during the open combustion of
785 biomass in the laboratory, *Journal of Geophysical Research-Atmospheres*, *114*,
786 doi:10.1029/2009jd011836.

787 Morgan, W. T., J. D. Allan, K. N. Bower, G. Capes, J. Crosier, P. I. Williams, and H. Coe (2009),
788 Vertical distribution of sub-micron aerosol chemical composition from North-Western Europe and the
789 North-East Atlantic, *Atmospheric Chemistry and Physics*, *9*(15), 5389-5401, doi:10.5194/acp-9-5389-
790 2009.

791 Morgan, W. T., J. D. Allan, K. N. Bower, E. J. Highwood, D. Liu, G. R. McMeeking, M. J.
792 Northway, P. I. Williams, R. Krejci and H. Coe (2010), Airborne measurements of the spatial
793 distribution of aerosol chemical composition across Europe and evolution of the organic fraction,
794 *Atmospheric Chemistry and Physics*, *10*(8), 4065-4083, doi: 10.5194/acp-10-4065-2010.

795 Ng, N. L., et al. (2010), Organic aerosol components observed in Northern Hemispheric datasets from
796 Aerosol Mass Spectrometry, *Atmospheric Chemistry and Physics*, *10*(10), 4625-4641,
797 doi:10.5194/acp-10-4625-2010.

798 Nowak, J. B., J. A. Neuman, K. Kozai, L. G. Huey, D. J. Tanner, J. S. Holloway, T. B. Ryerson, G. J.
799 Frost, S. A. McKeen, and F. C. Fehsenfeld (2007), A chemical ionization mass spectrometry

technique for airborne measurements of ammonia, *Journal of Geophysical Research-Atmospheres*, *112*(D10), doi:10.1029/2006jd007589.

O'Shea, S. J., et al. (2013_a), Airborne observations of trace gases over boreal Canada during BORTAS: campaign climatology, airmass analysis and enhancement ratios, *Atmospheric Chemistry and Physics*, *13*, 12451-12467, doi:10.5194/acp-13-12451-2013.

O'Shea, S. J., S. J. B. Bauguitte, M. W. Gallagher, D. Lowry, and C. J. Percival (2013_b), Development of a cavity-enhanced absorption spectrometer for airborne measurements of CH4 and CO2, *Atmospheric Measurement Techniques*, *6*(5), 1095-1109, doi:10.5194/amt-6-1095-2013.

Palmer, P. I., et al. (2013), Quantifying the impact of BOReal forest fires on Tropospheric oxidants over the Atlantic using Aircraft and Satellites (BORTAS) experiment: design, execution and science overview, *Atmospheric Chemistry and Physics*, *13*(13), 6239-6261, doi:10.5194/acp-13-6239-2013.

Parrington, M., et al. (2012), The influence of boreal biomass burning emissions on the distribution of tropospheric ozone over North America and the North Atlantic during 2010, *Atmospheric Chemistry and Physics*, *12*(4), 2077-2098, doi:10.5194/acp-12-2077-2012.

Parrington, M., et al. (2013), Ozone photochemistry in boreal biomass burning plumes, *Atmospheric Chemistry and Physics*, *13*(15), 7321-7341, doi:10.5194/acp-13-7321-2013.

Petzold, A., et al. (2007), Perturbation of the European free troposphere aerosol by North American forest fire plumes during the ICARTT-ITOP experiment in summer 2004, *Atmospheric Chemistry and Physics*, *7*(19), 5105-5127.

Reid, J. S., and P. V. Hobbs (1998), Physical and optical properties of young smoke from individual biomass fires in Brazil, *Journal of Geophysical Research-Atmospheres*, 103(D24), 32013-32030.

Reid, J. S., R. Koppmann, T. F. Eck, and D. P. Eleuterio (2005), A review of biomass burning emissions part II: intensive physical properties of biomass burning particles, *Atmospheric Chemistry and Physics*, *5*, 799-825.

Schneider, J., S. Weimer, F. Drewnick, S. Borrmann, G. Helas, P. Gwaze, O. Schmid, M. O. Andreae, and U. Kirchner (2006), Mass spectrometric analysis and aerodynamic properties of various types of combustion-related aerosol particles, *International Journal of Mass Spectrometry*, *258*(1-3), 37-49, doi:10.1016/j.ijms.2006.07.008.

Schwarz, J. P., et al. (2006), Single-particle measurements of midlatitude black carbon and light-scattering aerosols from the boundary layer to the lower stratosphere, *Journal of Geophysical Research-Atmospheres*, *111*(D16), doi:10.1029/2006jd007076.

Simoneit, B. R. T., J. J. Schauer, C. G. Nolte, D. R. Oros, V. O. Elias, M. P. Fraser, W. F. Rogge, and G. R. Cass (1999), Levoglucosan, a tracer for cellulose in biomass burning and atmospheric particles, *Atmospheric Environment*, *33*(2), 173-182, doi:10.1016/s1352-2310(98)00145-9.

Sinha, P., P. V. Hobbs, R. J. Yokelson, I. T. Bertschi, D. R. Blake, I. J. Simpson, S. Gao, T. W. Kirchstetter, and T. Novakov (2003), Emissions of trace gases and particles from savanna fires in southern Africa, *Journal of Geophysical Research-Atmospheres*, *108*(D13), 32, doi:10.1029/2002jd002325.

Slowik, J. G., et al. (2010), Characterization of a large biogenic secondary organic aerosol event from eastern Canadian forests, *Atmospheric Chemistry and Physics*, *10*(6), 2825-2845.

840 Sullivan, A. P., A. S. Holden, L. A. Patterson, G. R. McMeeking, S. M. Kreidenweis, W. C. Malm,
841 W. M. Hao, C. E. Wold, and J. L. Collett, Jr. (2008), A method for smoke marker measurements and
842 its potential application for determining the contribution of biomass burning from wildfires and
843 prescribed fires to ambient PM2.5 organic carbon, *Journal of Geophysical Research-Atmospheres*,
844 *113*, doi:10.1029/2008jd010216.

845 Taylor, J. W., et al. (2014), Size-dependent wet removal of black carbon in Canadian biomass burning
846 plumes, *Atmospheric Chemistry and Physics*, *14*, 13755-13771, doi:10.5194/acp-14-13755-2014.

847 Textor, C., et al. (2006), Analysis and quantification of the diversities of aerosol life cycles within
848 AeroCom, *Atmospheric Chemistry and Physics*, *6*, 1777-1813.

849 Vay, S. A., et al. (2011), Patterns of CO2 and radiocarbon across high northern latitudes during
850 International Polar Year 2008, *Journal of Geophysical Research-Atmospheres*, *116*,
851 doi:10.1029/2011jd015643.

852 Warneke, C., et al. (2006), Biomass burning and anthropogenic sources of CO over New England in
853 the summer 2004, *Journal of Geophysical Research-Atmospheres*, *111*(D23),
854 doi:10.1029/2005jd006878.

855 Weimer, S., M. R. Alfarra, D. Schreiber, M. Mohr, A. S. H. Prevot, and U. Baltensperger (2008),
856 Organic aerosol mass spectral signatures from wood-burning emissions: Influence of burning
857 conditions and wood type, *Journal of Geophysical Research-Atmospheres*, *113*(D10),
858 doi:10.1029/2007jd009309.

859 Yokelson, R. J., R. Susott, D. E. Ward, J. Reardon, and D. W. T. Griffith (1997), Emissions from
860 smoldering combustion of biomass measured by open-path Fourier transform infrared spectroscopy,
861 *Journal of Geophysical Research-Atmospheres*, *102*(D15), 18865-18877, doi:10.1029/97jd00852.

862 Yokelson, R. J., et al. (2007), Emissions from forest fires near Mexico City, *Atmospheric Chemistry*
863 *and Physics*, *7*(21), 5569-5584.

864 Yokelson, R. J., et al. (2009), Emissions from biomass burning in the Yucatan, *Atmospheric*
865 *Chemistry and Physics*, *9*(15), 5785-5812.

866 Zhang, Q., D. R. Worsnop, M. R. Canagaratna, and J. L. Jimenez (2005), Hydrocarbon-like and
867 oxygenated organic aerosols in Pittsburgh: insights into sources and processes of organic aerosols,
868 *Atmospheric Chemistry and Physics*, *5*, 3289-3311.

869 Zhang, Q., et al. (2007), Ubiquity and dominance of oxygenated species in organic aerosols in
870 anthropogenically-influenced Northern Hemisphere midlatitudes, *Geophysical Research Letters*,
871 *34*(13), doi:10.1029/2007gl029979.

872

Figures

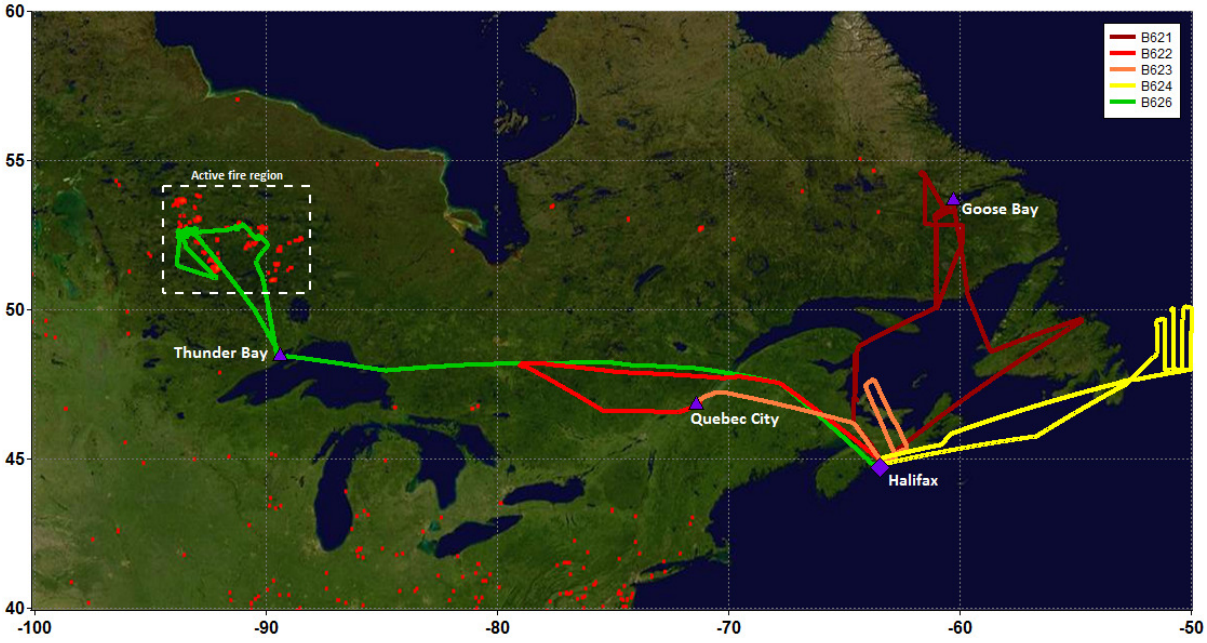

Figure 1: Flight tracks for flights B621-624 and B626 during BORTAS, overlain on a MODIS accumulated 10 day fire map for eastern Canada during the period 20/07/2011 – 29/07/2011. Images courtesy of MODIS Rapid Response Project at NASA/GSFC.

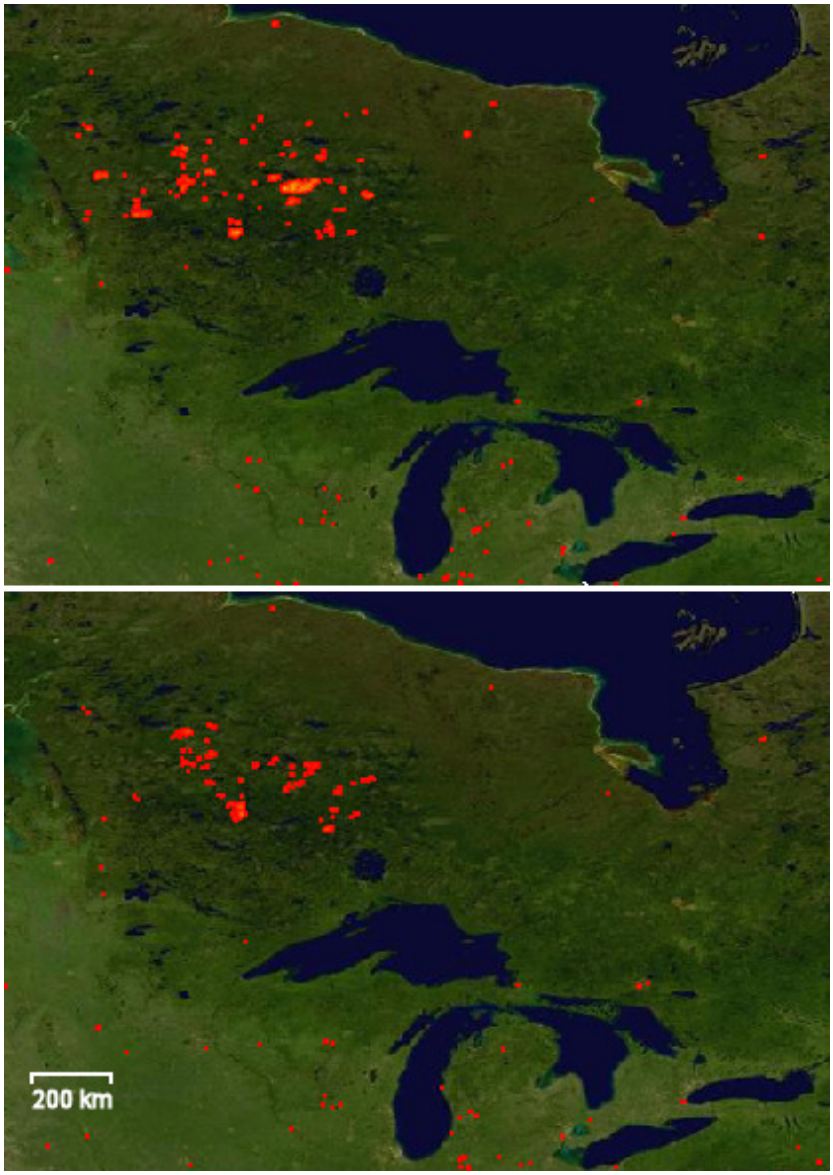

Figure 2: MODIS fire maps showing the reduction in fire activity in northwestern Ontario between the 10 day periods of 10/07/2011 – 19/07/2011 (top) and 20/07/2011 – 29/07/2011 (bottom).

883

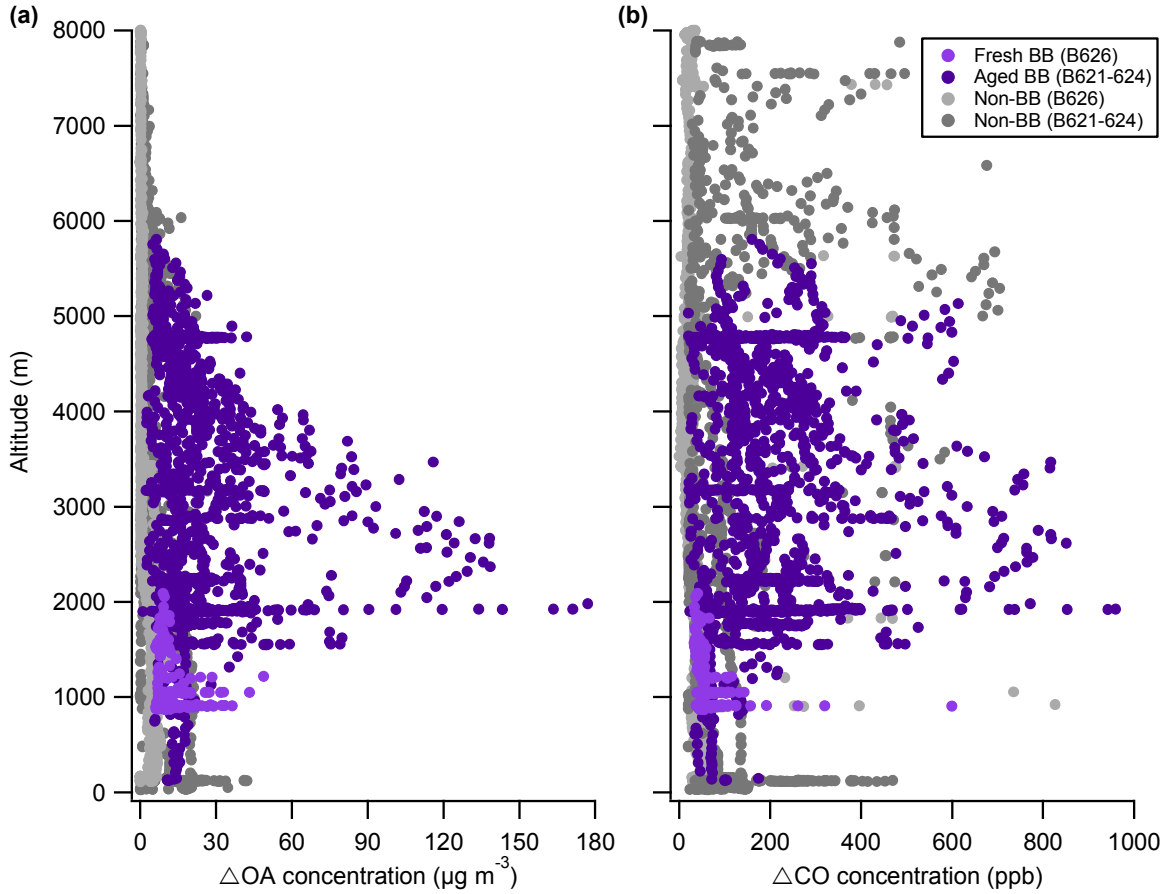

884

885 Figure 3: Vertical profiles of (a) △OA and (b) △CO in fresh and aged plumes, together with
886 concentrations in air masses free from the influence of biomass burning.

887

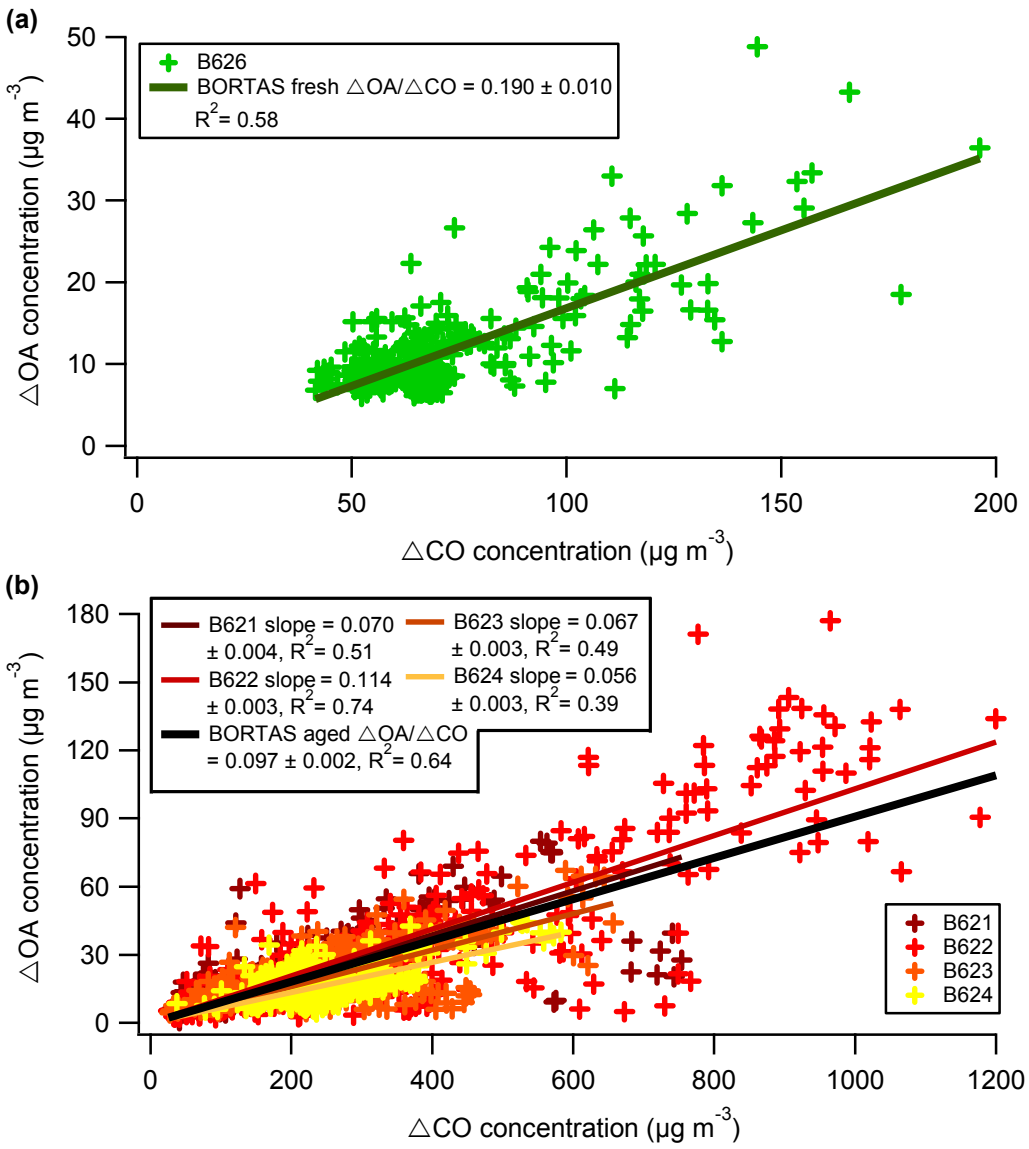

Figure 4: △OA versus △CO for (a) fresh and (b) aged plumes. Coefficients are for linear regressions, from which average △OA/△CO ratios are derived, with uncertainties of ± 1σ.

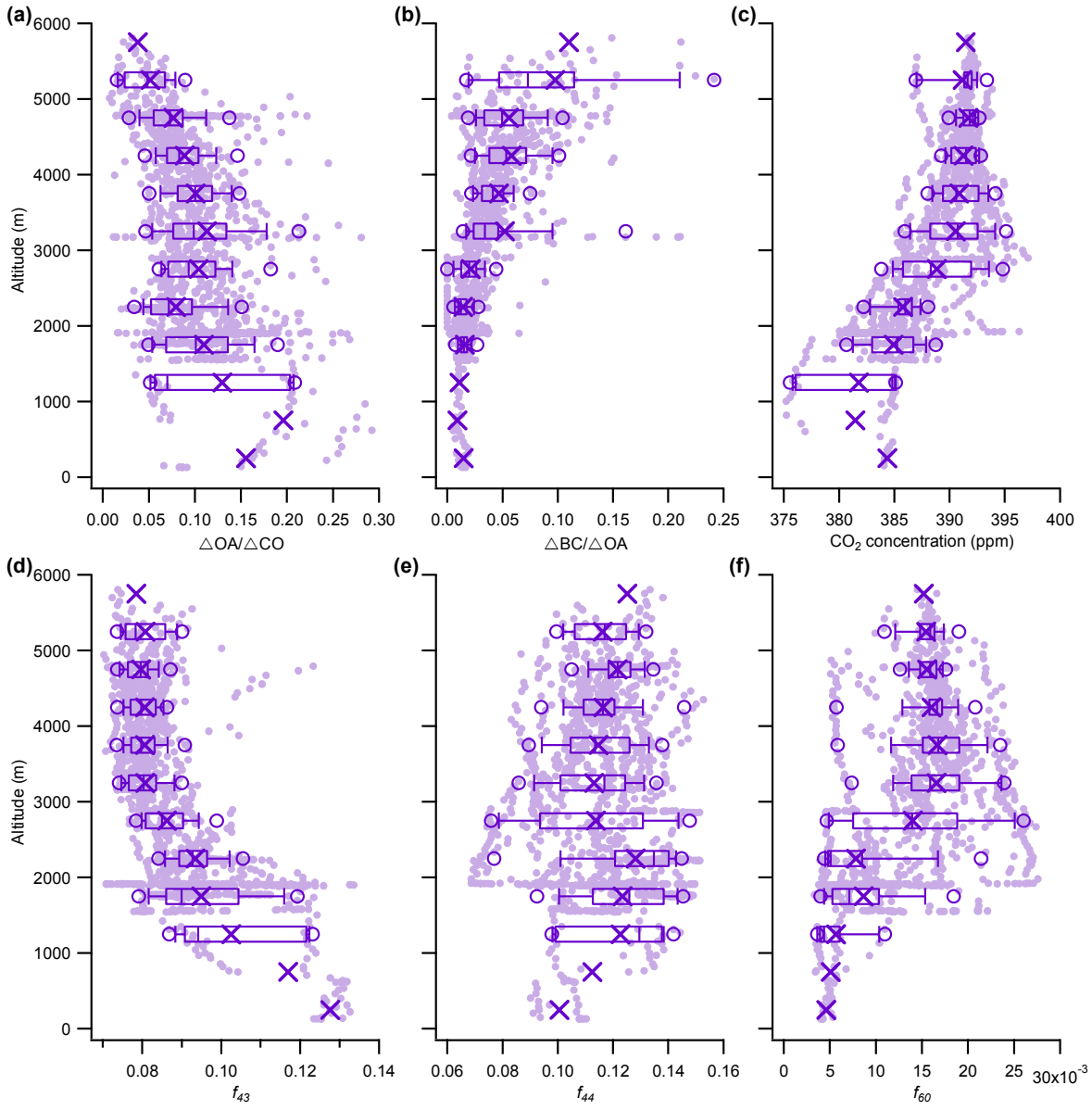

Figure 5: Vertical profiles of (a) △OA/△CO, (b) △BC/△OA, (c) CO_2, (d) f_{43}, (e) f_{44} and (f) f_{60} in aged plumes. Circles represent the 5th and 95th percentiles, vertical lines the 10th, 25th, 50th, 75th and 90th percentile, with crosses denoting mean values in each 500 m altitudinal bin.

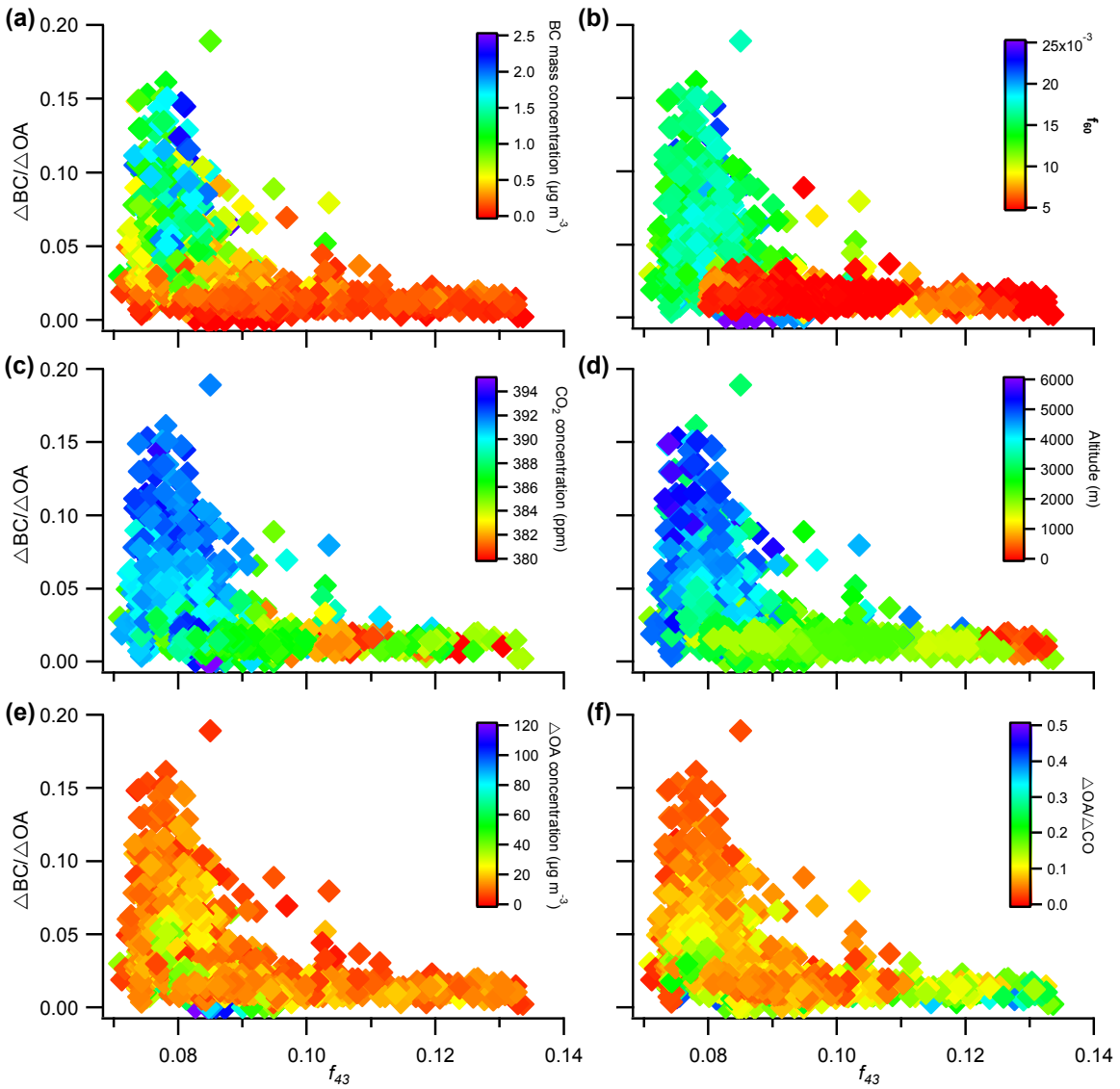

Figure 6: △BC/△OA versus f_{43} for aged emissions. Datapoints are coloured to show relationships with (a) △BC, (b) f_{60}, (c) CO_2, (d) altitude, (e) △OA and (f) △OA/△CO.

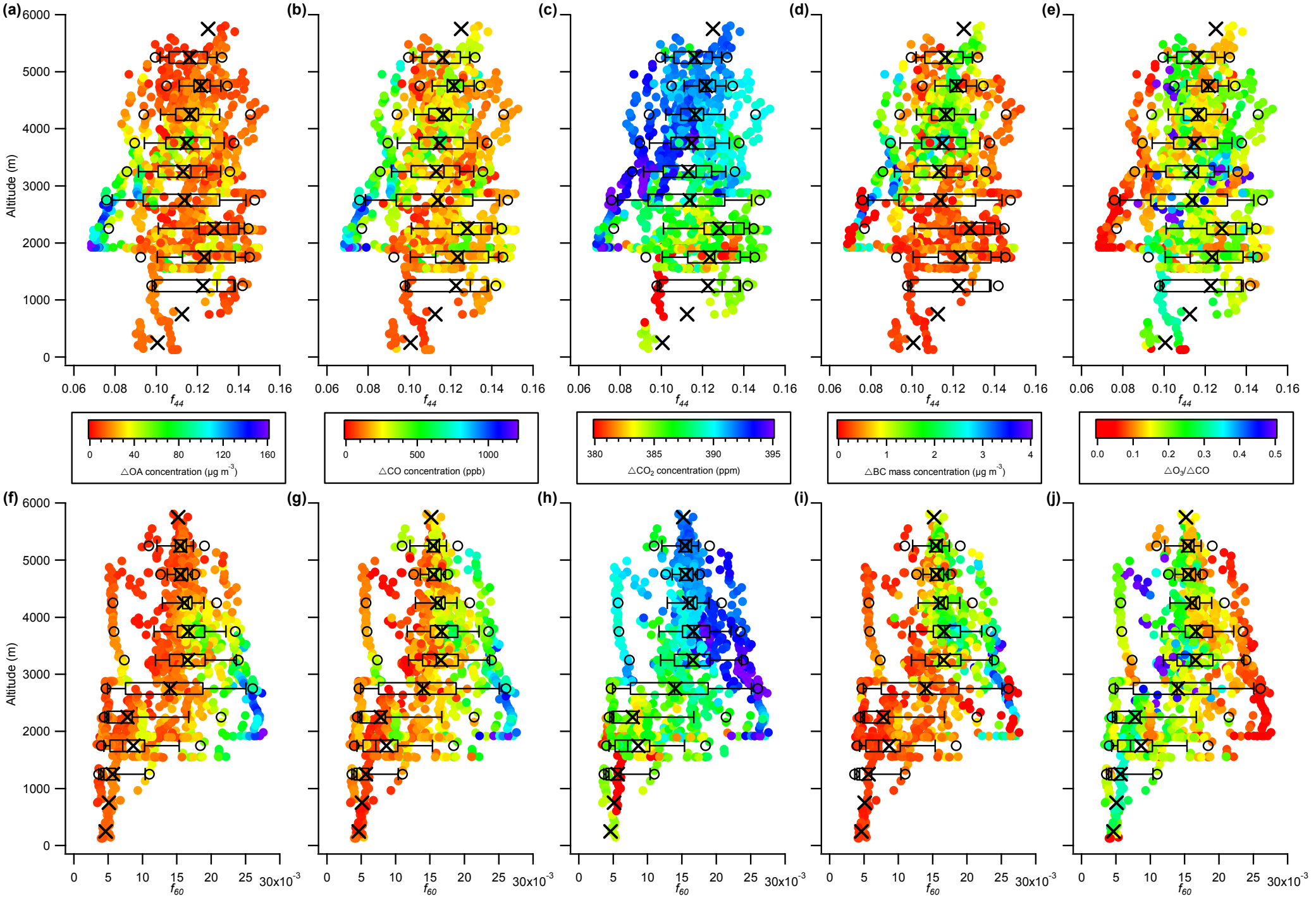

Figure 7: Vertical profiles of (a-e) f_{44} and (f-j) f_{60} in aged plumes. Datapoints are coloured by (a+f) △OA, (b+g) △CO, (c+h) CO_2, (d+i) △BC and (e+j) △O_3/△CO. Circles represent the 5th and 95th percentiles, vertical lines the 10th, 25th, 50th, 75th and 90th percentile, with crosses denoting mean values in each 500 m altitudinal bin.

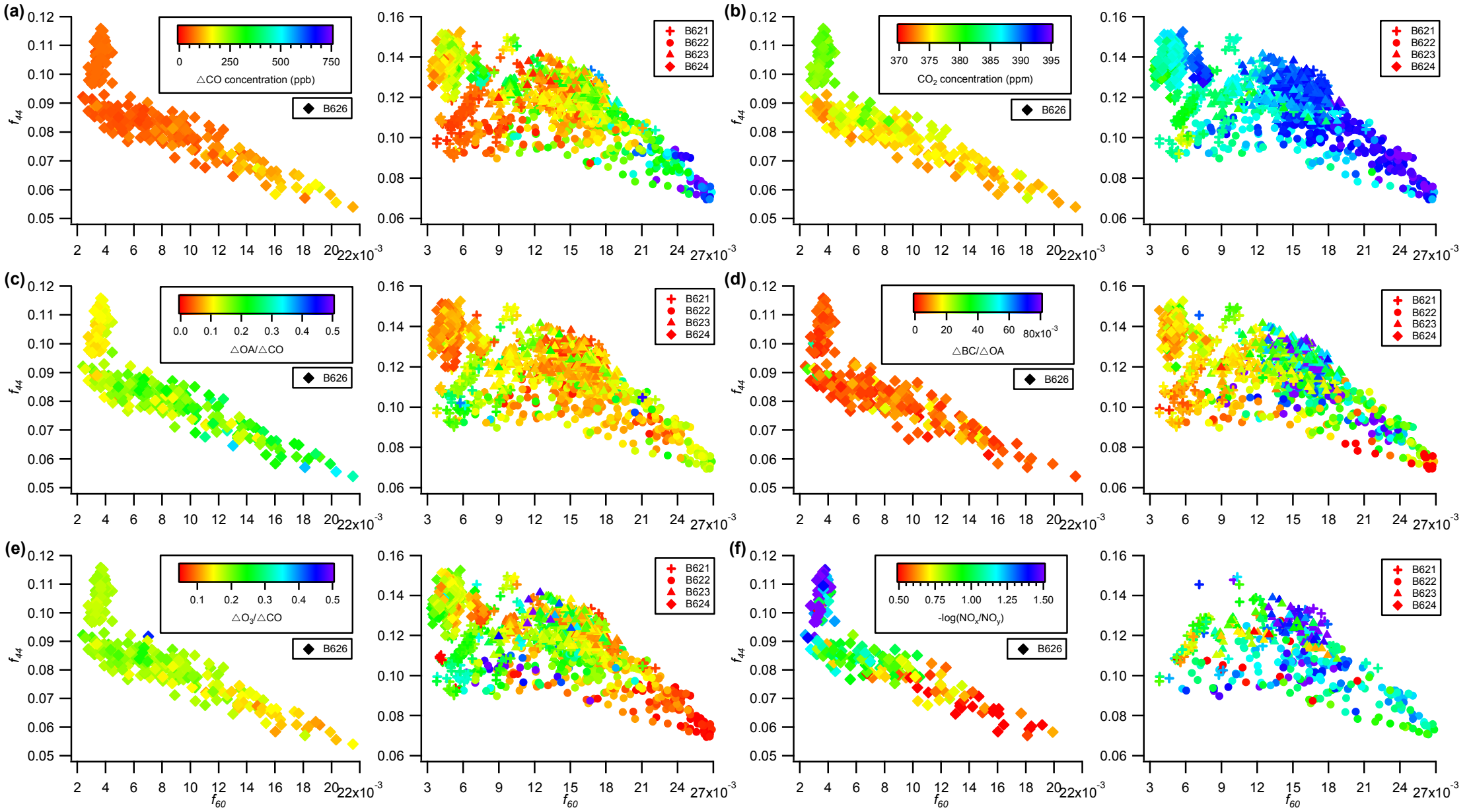

Figure 8: f_{44} versus f_{60} with datapoints coloured by (a) △CO, (b) CO_2, (c) △OA/△CO, (d) △BC/△OA, (e) △O_3/△CO and (f) -log(NO_x/NO_y). Data from fresh and aged plumes are shown on the left and right hand side of each panel, respectively.

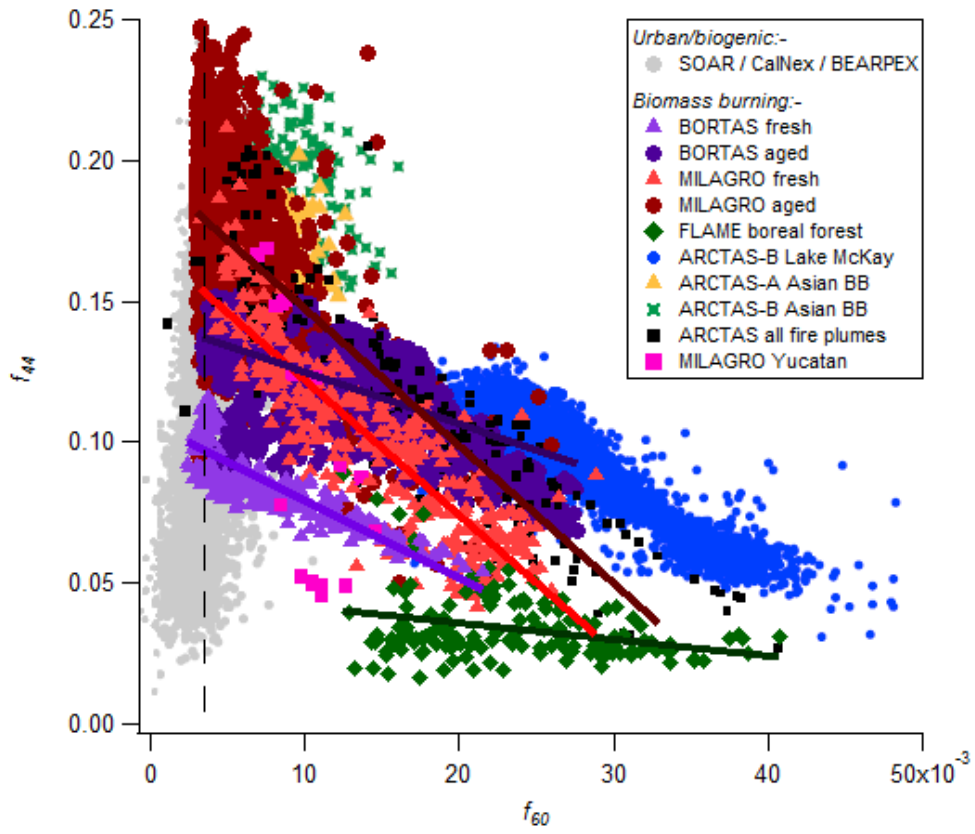

Figure 9: Synthesis of f_{44} versus f_{60} from a range of ambient and laboratory measurements of BBOA, along with data from non-BB sources. The specified background f_{60} value of 0.003 used to identify BB influences is shown as the dashed vertical line. Coloured lines denote linear regressions for corresponding datasets. Adapted from *Cubison et al.* (*2011*).

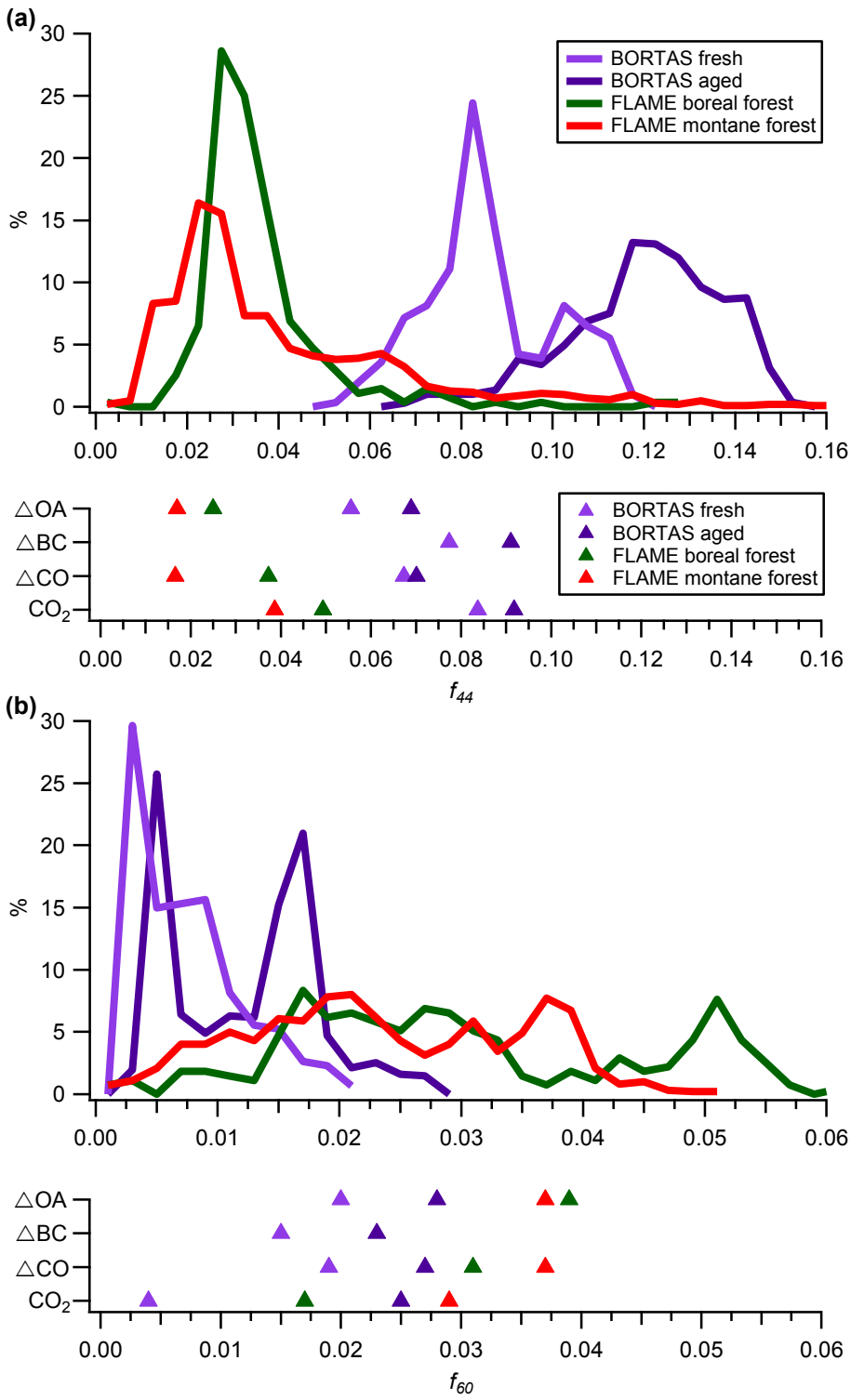

Figure 10: Probability density functions for (a) f_{44} and (b) f_{60} from a range of ambient and laboratory BB measurements. Also shown in the lower sections of each panel are the f_{44} and f_{60} values corresponding to maximum concentrations of △OA, △BC, △CO and CO_2.